MDPI

Review

A Systematic Review of the Recent Advances in Superlubricity Research

Qunfeng Zeng * and **Wenling Zhang**

Key Laboratory of Education Ministry for Modern Design and Rotor-Bearing System, Xi'an Jiaotong University,
Xi'an 710049, China; zwl203450@163.com
* Correspondence: zengqf1949@gmail.com

Abstract: Friction and the wear caused by friction will not only lead to energy dissipation, but will also cause damage to the function of mechanical parts, affecting the precision and lifespan of mechanical devices. Superlubricity as an ideal state of zero friction has become a hot research topic in recent years. There have been many reviews on the concept, origin, and research progress of superlubricity, but, among them, there are more presentations on the research status of solid superlubricity and liquid superlubricity; however, the theoretical summarization of solid–liquid combined superlubricity and high-temperature superlubricity is still imperfect and lacks a systematic and comprehensive review. The mechanism of superlubricity is not explicitly presented in many reviews, which are clearly summarized in this paper. This paper introduces superlubricity from friction, and then introduces the origin of superlubricity, and presents the research progress on superlubricityby separating it into in four categories: liquid superlubricity, solid superlubricity, solid–liquid combined superlubricity, and high-temperature superlubricity. By analyzing the superlubricity system, the mechanism of realizing various types of superlubricity, such as incommensurability, hydration, and oxidation, is summarized. Based on the research progress of superlubricity, the development prospects, opportunities, and challenges of superlubricity in the future are discussed.

Keywords: solid superlubricity; liquid superlubricity; solid–liquid superlubricity; high-temperature superlubricity; superlubricity application

1. Introduction

Friction is a very common physical phenomenon in life, occurring widely between surfaces that are in contact and in relative motion or that have a tendency to move, and it is involved in many fields, such as machinery, aerospace, transportation, marine, chemical industry, bioengineering, and so on. Thanks to friction, we are able to utilize it to perform tasks that improve our lives, but at the same time the presence of friction also leads to energy dissipation, and induces material migration on the surfaces of the moving parts, which leads to wear and tear and ultimately to the degradation or even loss of functionality of the parts. Lubrication failure and excessive wear often occur in mechanical components. Therefore, it is crucial to enhance the friction state between mechanical parts and efficiently decrease the coefficient of friction. According to statistics, friction consumes 1/3 of the world's disposable energy, about 80% of mechanical parts fail because of wear, and more than 50% of the vicious accidents due to mechanical equipment are caused by lubrication failure, resulting in losses of about 5% of the gross national product of the industrial society, which is extremely costly to resources, the environment, and the economy in today's world [1]. With the rapid industrial development, the contradiction between the sharp increase in energy consumption and the lack of resources is becoming more and more serious. Friction, as an important way to consume energy and promote the progress of tribology in order to boost green and sustainable energy development, has become crucial.

Superlubricity technology is currently a crucial solution for overcoming issues related to friction and wear. Its emergence offers significant improvements regarding the energy utilization efficiency of motion systems. What is commonly called superlubricity can be thought of as a state of lubrication in which the friction between two surfaces in contact is close to zero. In fact, the scientific concept of superlubricity is not yet clear in the academic and engineering communities. Due to signal interference, the current friction test instrument is often unable to accurately measure the friction coefficient if it is less than 10^{-4} and its following friction state [2], so the lubrication state with a friction coefficient of 10^{-3} or lower is usually called superlubricity [3]. According to its characteristics, it is mainly divided into solid superlubricity, liquid superlubricity, and solid–liquid combined superlubricity.

Superlubricity, as a brand new research direction in tribology, has attracted increasing interest since it was first proposed. In the past decades, remarkable progress has been made in this field, and there has been extensive research leading to an in-depth understanding of superlubricity. In this paper, we introduce the origin, realization, mechanism, and materials with properties of superlubricity. We also summarize the latest research progress in superlubricity both domestically and internationally and discuss its future applications.

2. The Development of Superlubricity

2.1. Origin of Superlubricity

The origin of the superlubricity phenomenon can be traced back to the early 1990s. The Japanese scholars Hirano and Shinjo found through theoretical calculation that when two crystal planes move in certain directions, the friction between the crystal planes will completely disappear when they are in an incommensurable state, which is called "superlubricity" [4]. However, if the crystal size and orientation of the two sliding surfaces are exactly the same, that is, the microstructure is in a commensurable state, the superlubricity will disappear, as shown in Figure 1. In view of the fact that the ultra-low friction produced by the incommensurate contact interface mainly comes from the geometric structure effect under the interface mismatch, the scholar Müser [5,6] suggested that the discovery of Hirano et al. [7–9] should be called "structural lubrication" or "structural superlubricity". In addition, it was found that for the rigid sliding system, under the condition of low load, interface sliding can easily avoid the "stick-slip" sliding mode with high energy dissipation and realize continuous sliding [10]. This extremely low friction state is also customarily called "superlubricity" [11–13]. Energy dissipation is the basic principle used to measure the friction resistance caused by the relative movement of the material interface, and the existence of sliding barriers is the key reason for the dissipation and friction caused by interface sliding. Although there are differences between superlubricity and ultra-low friction in principle, both of them follow the general principle of reducing the interface sliding energy barrier to achieve low friction. Subsequently, many scholars have carried out research on superlubricity because once friction can disappear, human beings will benefit a lot. On the one hand, people explore the realization conditions and mechanism of superlubricity state in theory; on the other hand, they look for materials with superlubricity characteristics in experiments [1]. At present, structural superlubricity and ultra-low friction are important methods to obtain a super-lubrication state in current academic circles, among which structural superlubricity may be one of the more widely studied methods.
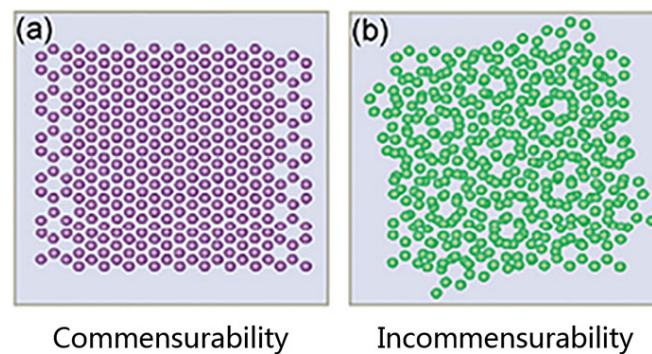
Figure 1. Two graphene layers in contact in commensurate registry (**a**) and in incommensurate registry (**b**) [14].

2.2. Research Status of Superlubricity

2.2.1. Liquid Superlubricity

Liquid lubrication is one of the main means of reducing friction. Unlike the friction mechanism described in solid superlubricity, the main source of friction in liquid lubrication is the internal friction of the fluid, which, according to the lubrication theory, can be reduced by reducing the viscosity of the lubricant. However, as the viscosity of the lubricant decreases, so does its load-carrying capacity, and so it is not feasible to significantly reduce friction in this way. Therefore, tribologists have been working in this field for a long time, trying to find practical ways to significantly reduce friction. Liquid lubricants mainly include two kinds: oil-based and water-based. For oil-based lubricants, they are characterized by a high viscosity and high coefficient of viscous pressure, so it is easy to form fluid lubrication between the surfaces of the friction pair. The lowest friction coefficient corresponding to traditional oil-based lubricants is usually between 0.01 and 0.05, mainly due to the limitations of their viscosity. For water-based lubricant, it has the characteristics of low viscosity and a small coefficient of viscous pressure, so the lubrication between the friction parts is often in the form of boundary lubrication or mixed lubrication [15].
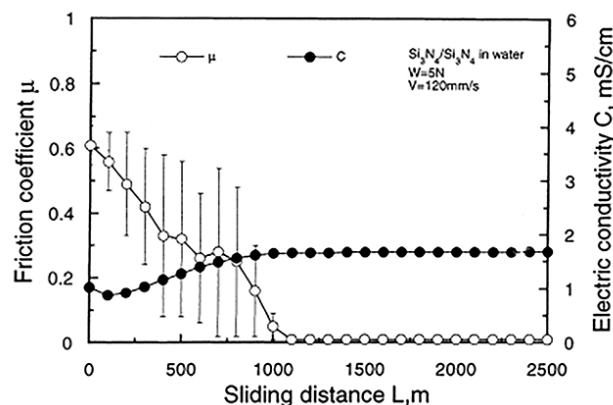
(1)   Water-based lubrication

In 1987, Tomizawa and Fischer [16] found a silicon nitride ceramic (Si_3N_4) in the water as a lubricant under the conditions of a period of break-in. Its final coefficient of friction was less than 0.002, demonstrating, for the first time, that water can achieve superlubricity as a lubricant [17], as shown in Figure 2. Subsequently, many scholars have begun to study the system of ceramic water lubrication, and found that other types of ceramics, such as silicon carbide ceramics (SiC) and alumina ceramics (Al_2O_3), after a break-in period, can also be obtained with an ultra-low friction coefficient of less than 0.01. Related experiments have shown that ceramic surfaces undergo friction chemical reactions with water molecules during the break-in process:

$$Si_3N_4 + 6H_2O = 3SiO_2 + 4NH_3 \tag{1}$$

$$SiO_2 + 2H_2O = Si(OH)_4 \tag{2}$$

$$Si(OH)_4 = H^+ + H_3SiO_4^- \tag{3}$$
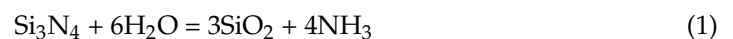
This forms a negatively charged layer of silica sol on the surface of the friction pair. In the presence of an electric charge, a Stern layer and a double electric layer are formed on the surface of the silica sol [18,19]. When the silica sols are in contact with each other, their shear strength is very low, which results in a small coefficient of friction for boundary lubrication. And due to the existence of the fluid dynamic pressure effect, a layer of water film will also be formed between the silica sols, and the friction coefficient of the fluid dynamic pressure lubrication formed is also very small due to the low viscosity of water.

Therefore, they concluded that the ceramic friction pair forming superlubricity is located in the mixed lubrication region (boundary lubrication and fluid lubrication), so that a very low coefficient of friction can be realized [15,20].

Figure 2. Friction coefficient variation curve and conductivity curve of Si3N4/Si3N4 friction pair under water lubrication conditions [21].

(2)   Polymer fluid lubrication

The second class of water-based lubricants with superlubricity properties is the polymer molecular brushes [22], i.e., the polar end of the polymer is grafted onto the surface, and the other end of the long chain floats in the water to form a layer of molecular brushes, as shown in Figure 3. Because the long chain can be stretched well in the solvent without detaching from the surface, the molecular brush can produce a strong penetration pressure between the polymer brush and the double electric layer repulsive force and dispersive force. For the polymer between the force field in the repulsive field range and in the molecular brush under the action of the huge repulsive force, even at a higher pressure (1 MPa), the two surfaces are still separated by molecular brushes, resulting in a coefficient of friction of the order of 0.001 [23]. Since the 1990s, Klein et al. [24] have carried out a lot of research on the superlubricity of polymer molecular brushes by using a surface force apparatus. They formed polymer molecular brushes on two mica surfaces via electro static adsorption, and the friction coefficients between them could reach a 0.001 order of magnitude or even lower, and, later on, using brine as a lubricant between the mica, friction coefficients of up to a 0.0001 order of magnitude could be realized, being attributed to the results of hydration. At the same time, their research found that when water is used as lubricant, charged polymers (such as polyelectrolyte) have better lubrication characteristics than other polymers and can achieve an ultra-low friction coefficient less than 0.0006 under a pressure of 0.3 MPa. They proposed that there are a lot of moving ions with opposite charges in the molecular brush layer formed by charged polymers, and that the potential generated by these ions to inhibit the interpenetration between molecular brushes will be much stronger than that of neutral molecular brushes. This means that the interpenetration between charged molecular brushes can be suppressed, which greatly reduces the energy dissipation and thus reduces the friction resistance of the system [25,26]. However, for polymer molecular brushes, it is only possible to obtain superlubricity on the surface force apparatus (low speed and low load), and it is very difficult to realize superlubricity under macroscopic conditions, so its application to mechanical systems is greatly limited [27].
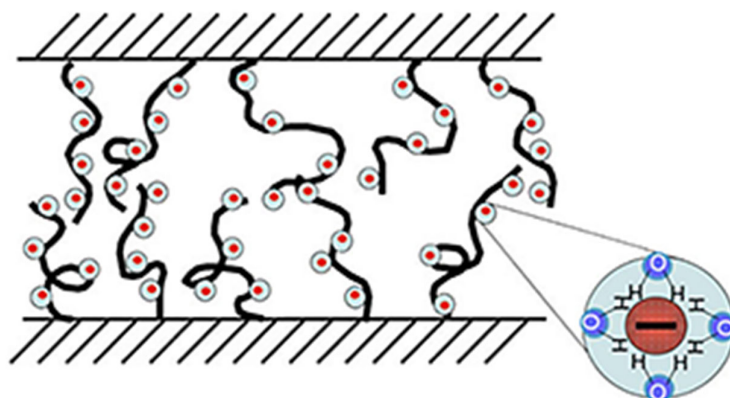
Figure 3. Schematic of the lubrication of a charged polymer confined between two mica [28].

(3)   Acid-based liquid

However, the realization of liquid superlubricity under macro conditions (high speed and high load) is a difficult problem because it requires not only the inability of liquid molecules to be squeezed out of the contact zone under high pressure, but also that liquid molecules have a small shear strength [15]. This problem gave rise to the study of acid-based solutions to achieve macroscopic superlubricity. First, the team of Luo Jianbin found that phosphoric acid with pH=1.5 could help to realize superlubrication under the conditions of a load of 3N (maximum contact pressure of 700 MPa), a linear speed of 0.057m/s, and a friction coefficient between glass/silicon nitride and sapphire/sapphire surfaces of 0.004 after 10 min of operation [29]. Relevant experiments show that phosphoric acid superlubricity is closely related to the hydrogen ions in solution and the structure of the hydrogen bonding network formed between phosphoric acid and water molecules [30]. Based on the analysis, a model of superlubricity of phosphoric acid was established. When superlubricity occurs, the contact zone is a three-layer structure: a Stern layer, an adsorption membrane with a hydrogen bonding network structure, and a layer of free water molecules. The main function of the Stern layer is to connect the hydrogen bond network structure with the surface of the friction pair. The main function of the hydrogen bond network structure is to bear the load and keep the water molecules confined in the contact zone. The main function of the free water molecule layer is to provide very low shear strength. According to the above-mentioned phosphoric acid superlubricity model, Luo Jianbin and others infer that the realization of superlubricity needs to meet at least two conditions: ① hydrogen ion, which can absorb on the surface of a friction pair to charge the surface and form a Stern layer; and ② hydrogen bonding, which can form a hydrogen bonding network structure and fix water molecules in the contact zone. Therefore, if we have these two characteristics in other experimental schemes, we should also have superlubricity. In the mixture of acid and glycerol, superlubricity was quickly realized via a similar scheme, which further proved the above theory [31]. Of course, acid is at the same time a double-edged sword, and the problem with the acid-assisted realization of superlubricity is obvious: the presence of acid can easily cause the corrosion of the friction pair surface. Later, Ge Xiangyu et al. demonstrated that a similar state of superlubricity could be achieved under neutral conditions (pH $\approx$ 6.4) when boric acid was added to an aqueous solution of poly(ethylene glycol) (PEG). Boric acid reacts with polyethylene glycol to form boron chelates, a process that not only neutralizes the solution but also provides a continuous supply of H^+ ions, which is key to the lubrication running process [32].

(4)   Oil-based lubrication

Commonly used oil-based lubricants are divided into vegetable oil, mineral oil, liquid paraffin, silicone oil, organic synthetic oil, and so on [33,34]. In 2017, Bouchet et al. added ultra-smooth tetrahedral amorphous carbon (ta-C) to petroleum under the conditions of acid lubrication and diamond-like carbon coating, and reached an ultra-low friction

coefficient of 0.003. The reason is that the lubricating oil promoted the tribochemical reaction of hydrogen-free carbon in ta-C due to the high initial sp3 content [35]. In 2013, Qunfeng Zeng et al. achieved a superlubricity phenomenon with a friction coefficient of 0.001 by using the addition of olefin oil to α-nano boron nitride particles [36]. Meanwhile, they also reported a novel superlubricity phenomenon: castor oil showed a superlubricity tendency (the friction coefficient could be as low as 0.0005) under the sliding friction of steel alloys [37]. In addition, Li Jinjinet al. achieved an ultra-low coefficient of friction of 0.005 by means of a steel/steel friction pair and in concert with a special 1,3-diketone lubricant [38]. The mechanism during lubrication is that the thickness of the layer gap between two shear surfaces is only a few tens of nanometer sthick, which makes the molecules undergo multiple shear motions within 10^{-6} s. Under such a strong shear effect, the effective viscosity of the member rotor in the friction gap and sliding direction is significantly reduced, which makes the whole lubrication state present in the film lubrication state. Their group chose silicone oil as the lubricant and utilized sulfuric acid to pretreat the silicon nitride/glass friction pair, which ultimately achieved superlubricity with a coefficient of friction of about 0.004, and the superlubricity life in this state can be guaranteed to be maintained for at least 5 h. It is worth noting that the coefficient of friction of silicone oil on the friction pair without sulfuric acid pretreatment is about 0.12, which is much higher than the former [39]. We know that the viscosity of the lubricant in general has a great influence on the coefficient of friction, but, at this time, the viscosity of the lubricant is insignificant to the coefficient of friction. The coefficient of friction of silicone oil with a friction partner utilizing sulfuric acid pretreatment is less than 0.01. This indicates that regardless of the viscosity of the silicone oil, sulfuric acid pretreatment is the key factor in achieving superlubricity with a silicon nitride/glass friction partner. In addition, if the increase in silicone oil viscosity is large, the coefficient of friction also increases, indicating that viscosity has an effect on fluid sliding. They suggest that the mechanism of superlubricity in lubrication systems works in that the acid solution helps to form a low-shear-resistance silicone oil-slip layer on the surface of silicon nitride during the break-in process, and therefore the contact pressure between the friction partners slowly decreases. Notably, this layer of silicone oil can form a fluid film that can easily shear in the contact area, which significantly reduces the coefficient of friction and ultimately achieves superlubricity.

(5)　Ionic liquid lubrication

Ionic fluids are a representative group of lubricants and lubricant additives that significantly reduce friction and wear and retard corrosion and mechanical failure. Room-temperature ionic liquids have a variety of excellent properties, including nonflammability, difficult volatility, a wide electrochemical window, high conductivity, and good thermal stability, and thus have attracted the attention of scholars in both basic research and applications [40]. In order to explore the superlubricity of ionic liquids, Ge Xiangyu et al. [41] comparatively investigated four aqueous solutions of ionic liquids on silicon nitride/silicon dioxide friction substitutes, among which the friction coefficient of the [EMIM] TFS (aq) solution could reach 0.002 to achieve macroscopic superlubricity, and it was found that the superlubricity state could be stabilized for at least one hour, which is very stable under the natural conditions through observation and subsequent experiments. Since the four ionic liquids have the same cation, it is inferred that the superlubricity property of [EMIM] TFS (aq) is determined by its anion, which forms a layer of effective friction chemical film through the friction chemical reaction between the anion and the friction pair surface during the break-in stage, thus realizing superlubricity. T.I. Han et al. [42] obtained macroscopic superlubricity between silicon oxide spheres and sapphire disks at high pressure with the help of hydrated alkali metal ions, obtaining an ultra-low coefficient of friction of 0.005 at an average contact pressure of 0.25 GPa. In the boundary lubrication state, the hydrated shell layer wraps around the alkali metal ions like a protective shell, which provides a hydrated repulsive force to counterbalance large normal loads, provides a fluid response to shear, and significantly reduces friction.

(6) Organismal mucus lubrication

In addition to the liquid superlubricity mentioned above, there is also a class of biological materials that have superlubricity properties, such as certain organs in living organisms, human joints, human eyes, etc. This is mainly due to the existence of various different aqueous solutions of polymers between these organs, which are capable of providing excellent lubrication. For example, there is a polysaccharide polymer, hyaluronic acid, in human joints. Studies show that it can achieve an ultra-low friction coefficient of 0.003 between the two joints as a lubricant [43], so that we can walk without feeling joint pain. In addition, some types of plant mucus also have a good lubricating effect. In 2006, Arad et al. [44] extracted polysaccharides from red algae and achieved superlubricity. They attributed this superlubricity to the spiral chain structure, which can maintain a thin water layer inside under low load. Li Jinjin and others found that the mucus of an aquatic plant (Braseniaschreberi) could achieve superlubricity. The friction coefficient between it and the glass surface could be reduced to 0.005 at least [45]. The results show that there are many layered nanoflakes in the braseniaschreberi mucus, so they put forward a lubrication mechanism. In these polymers, nanoflakes combine with a large number of water molecules to form a hydration layer, which provides extremely low shear resistance and realizes superlubricity.

At present, most of the realization of the superlubricity state still needs a long break-in period. The long break-in period meansthat the friction vice may have already achieved serious wear before the superlubricity state was reached, so designing the lubrication material with a super short break-in period is also a difficult problem in this field. Recently, Wang Daoai's research team at the Lanzhou Institute of Chemistry designed and developed a variety of liquid superlubricity materials based on natural organic acids, and made progress in macro-scale liquid superlubricity research, shortening the running-in period to a few seconds [46]. Using the hydrogen bond interaction between tannic acid and polyethylene glycol, researchers developed a new type of environmentally friendly liquid superlubricity material, which can shorten the running-in period between silicon nitride and glass to 9s and the friction coefficient to as low as 0.005. In addition, researchers have discovered a new natural superlubricity material, plant water-soluble acid, the lubrication state of which can be maintained for at least 13h at low contact stress (0.4 MPa). Additionally, the lubricant can achieve rapid superlubricity between polydimethylsiloxane (PDMS) and a variety of friction pair materials, such as metals, polymers, and inorganic non-metals. Using an aqueous glycerol solution as a model, Qiang Ma et al. explained the mechanism of ultra-low friction through hydration lubrication in the hope of eliminating the long break-in period. The specific gravity of glycerin and water was varied in the experiments, and at a water/glycerin weight ratio of 2.0, the friction was initially high, and after a long break-in period, ultra-low friction was achieved. And when the water/glycerin specific gravity was reduced to 0.2, ultra-low friction was observed at the beginning of the test [47].

2.2.2. Solid Superlubricity

(1) MoS_2 lubrication

Since Hirano and Shinjo predicted super lubrication in 1990 [7], some of their early explorations have shown that there is a state of near-zero friction, and they considered incommensurability as the main mechanism to realize solid superlubricity [48,49]. Soon after, it was found that two-dimensional materials, such as molybdenum disulfide, boron nitride, graphite, and graphene, could feasibly obtain solid superlubricity. Because the interaction between two-dimensional materials was very weak and non-commensurability contact could be achieved, it provided conditions for realizing superlubricity. In 1993, Martin et al. [50] found that the friction coefficient of the molybdenum disulfide (MoS_2) layer was in the range of 0.001 under the ultra-high-vacuum condition. As shown in Figure 4, through the high-power transmission electron microscope, it can be seen that the molybdenum disulfide abrasive particles formed a neat pattern structure on the surface of the friction pair, which indicates that there are overlapping molybdenum disulfide crystals in the molybdenum disulfide abrasive particles, and that there is a rotation angle between

these crystals. Therefore, in the process of the mutual movement of crystals, the friction is anisotropic along the basal plane with high sulfur content, which is the fundamental reason why molybdenum disulfide has superlubricity, but molybdenum disulfide can only achieve an ultra-low friction coefficient under high-vacuum conditions, or under the protection of inert gases (such as pure nitrogen and argon). Under natural conditions, the existence of oxygen atoms and water vapor in the air prevents molybdenum disulfide from achieving super-sliding. In 2000, Chhowalla and Amaratunga [51] prepared a fullerene-structured MoS_2 thin film with super-smooth performance in an inert atmosphere and air with a humidity of 45%, and its friction coefficient reached 0.003. They thought that the curved S-Mo-S basal plane hindered the surface oxidation and protected the layered structure from being destroyed, so that the molybdenum disulfide could realize superlubricity under natural conditions.
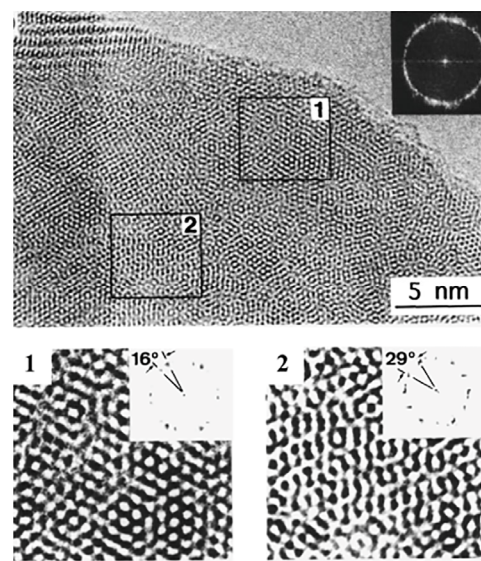

Figure 4. High-power transmission electron microscope diagram of molybdenum disulfide abrasive particles [50].

(2) Graphite lubrication (Experimental verification of superlubricity)

The concept of superlubricity has caused a lot of controversy since it was put forward. The biggest controversy is whether the concept of superlubricity is similar to the hot concepts of superconductivity and superfluidity at that time. In fact, the incommensurate crystal contact only cancels out one method of energy dissipation, that is, the stick-slip phenomenon in the low-speed sliding process, and there are other forms of energy dissipation in the sliding process, such as the generation of sound waves, which mean that the dynamic friction of even the most stringent incommensurate crystal contact in the experiment cannot reach zero. However, with the deepening of research, in 2004, M. Dienwiebel and others took the lead in observing the friction anisotropy between nano-graphite sheets and their structural superlubricity [52]. They glued a nano-graphite flake to the probe of a friction-force microscope and measured the friction force of the flake when sliding on the surface of highly oriented pyrolytic graphite (atomic smooth surface). The results showed that the friction force is extremely low (<50 pN) for most of the relative orientations of the sheet and the machine body, while the stick-slip motion is observed at this orientation angle when the orientation angle is very narrow (0 and 60, etc.), that is, incommensurate contact, and the friction force is large, as shown in Figure 5. This discovery is considered a milestone in the study of structural superlubricity. Following this, Verhoeven et al. theoretically explained the observed super-lubrication phenomenon through the extended Prandtl–Tomlinson model, in which the graphite flake was simplified to a rigid crystal plane with a finite size, as shown in Figure 6.
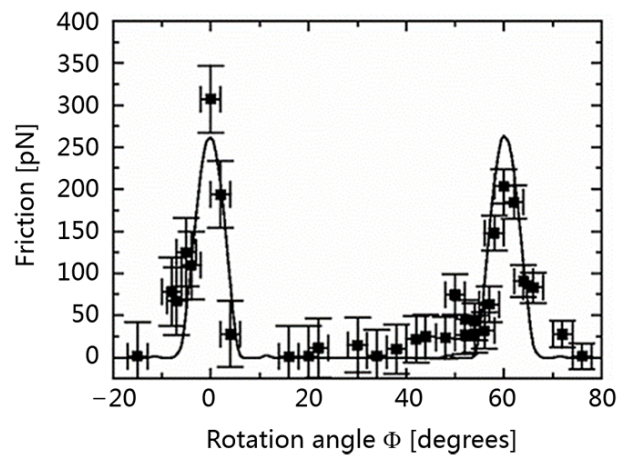
Figure 5. Friction forces (data points) at different rotation angles and friction forces (curves) calculated based on the PT model [52].
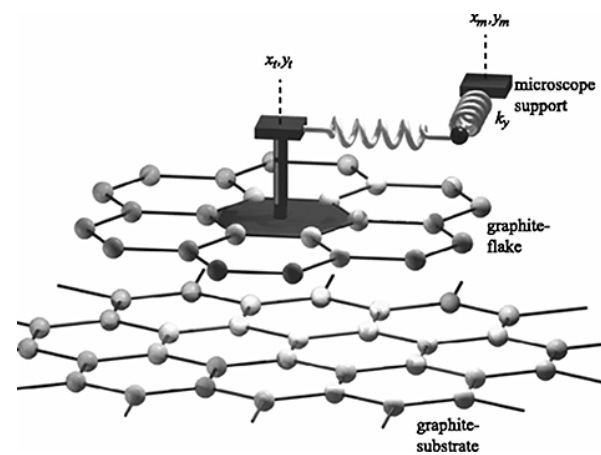
Figure 6. Schematic diagram of extended Prandtl–Tomlinson model used in super-lubrication simulation [53].

However, the nano-scale contact surface is too small compared with the scale required for practical application. Not to mention the macro-scale contact surface, and even the contact surface of the smallest bearing in the most precise mechanical watch has a scale of several hundred microns. The extension of nano-scale superlubricity to a micron or even a macro-scale is the premise of the practical application of superlubricity. However, the reality is cruel. The excitement about superlubricity research brought about by the breakthrough of superlubricity experiments in 2004 began to fade after several years. Until 2011, the reported superlubricity was still limited to a nano-scale, high-vacuum environment, and low speed (10 μm/s) [14], so the theoretical and experimental research related to superlubricity also gradually decreased. Scholars at home and abroad have put forward several different views on this issue. Among them, Dienwiebel and others, who have made a breakthrough in superlubricity in experiments [52–54], hold that superlubricity cannot be achieved on a larger scale, mainly because the crystal planes cannot achieve absolute stiffness, and the contact between the two crystal planes always tends to involve commensurability contact with lower energy. The deformation of the crystal plane will cause local congruence when the size of the contact surface is large, which will lead to the disappearance of superlubricity. The scholars represented by Zheng Quanshui's research team atTsinghua University hold another view. They believe that large-scale superlubricity can be realized, and it may not be affected by size. One of the important reasons for the failure of previous large-scale superlubricity attempts is that it is impossible to achieve absolutely clean crystal-face contact. When two originally separated crystal planes are

contacted by transfer, it is inevitable that there are adsorbents such as atoms, molecules, and nanoparticles on the crystal planes exposed to air (even in the ultra-clean room), so the contact formed in this way cannot be absolutely clean. However, according to the theoretical prediction made by American scholars M. Robbins and M. Mueser, the contact static friction force that is not absolutely clean is not zero [55,56]. So, achieving absolute clean contact in a large area is a very difficult problem. Another problem is that even if there is "zero" friction in the contact area, friction can be caused by many factors such as adsorption or deformation at the edge of the contact area, so it is difficult to distinguish whether these friction forces occur in the contact area or originate from the edge only by detecting the friction force.

Aimed at solving the above problems, Zheng Quanshui's research team [57] first observed the super-lubrication phenomenon on a micron scale through the ingenious graphite island self-retraction experiment in 2012. The phenomenon of self-retraction movement of the graphite island means that when the micron-scale highly oriented pyrolytic graphite (HOPG) island is sheared and dislocated, and when the external lateral force disappears, the sheared part will automatically retract to the original position on the graphite island, as shown in Figure 7. Through this experiment, they found that the friction obviously has the basic characteristics of superlubricity, that is, the friction is very small in the incommensurability orientation (the angle corresponding to the shadow in Figure 8j), and the friction is very large in some specific orientations (the direction of the blue arrow in Figure 8a–j) that are separated by about 60°, and the upper limit of the shear strength in the incommensurability orientation is only 0.04 MPa; however, the shear strength in commensurability is four orders of magnitude larger than that in incommensurability, which is about 140 MPa, so it can be concluded that this is a superlubricity phenomenon [57]. Moreover, the superlubricity phenomenon occurs in an atmospheric environment, and the maximum contact area reaches 10 μm × 10 μm [57], which is seven orders of magnitude larger than the results reported by other researchers. M. Hirano, the founder of superlubricity, and M. Urbakh, a famous nano-tribologist, think that this work is "a big step for the phenomenon of superlubricity to surpass the nanometer scale". Yang Jiarui and Zheng Quanshui invented a set of laser knife-edge detection equipment [58–61] (Figure 9). Using this equipment and highly oriented graphite, we found the phenomenon of superlubricity at a high speed (up to 25 m/s).
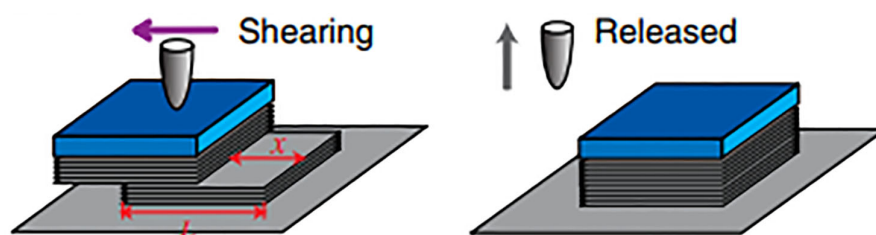

Figure 7. Schematic diagram of graphite island self-retraction [57].

(3)   DLC film lubrication

Another kind of superlubricity material is DLC (diamond-like carbon) film [59], which was first discovered by the Erdemir of Argonne Laboratory in the U.S. [60]. They obtained hydrogen-containing DLC films via plasma-enhanced chemical vapor deposition, which can achieve an ultra-low friction coefficient of 0.001. The research shows that whether the DLC film can achieve superlubricity is closely related to the hydrogen content in the film. As shown in Figure 10, the higher the hydrogen content in the gas atmosphere, the lower the friction coefficient of the DLC film. If the DLC film does not contain hydrogen, the friction coefficient is still high even under the protection of high vacuum or inert gas [61]. In recent years, some scholars have measured the friction coefficient of DLC films in a hydrogen atmosphere, and found that as long as there is enough hydrogen near the contact area, no matter how low the hydrogen content in DLC films is, it can always achieve a very low

friction coefficient [62]. These experimental results show that hydrogen atoms play a key role in the superlubricity process of DLC films. They think that hydrogen atoms combine with carbon atoms to form positively charged sliding surfaces, which have weak van der Waals forces and strong electrostatic repulsion, resulting in a low friction coefficient [63].

(Blue line)Self-locking direction   (Shadow)Superlubricity direction
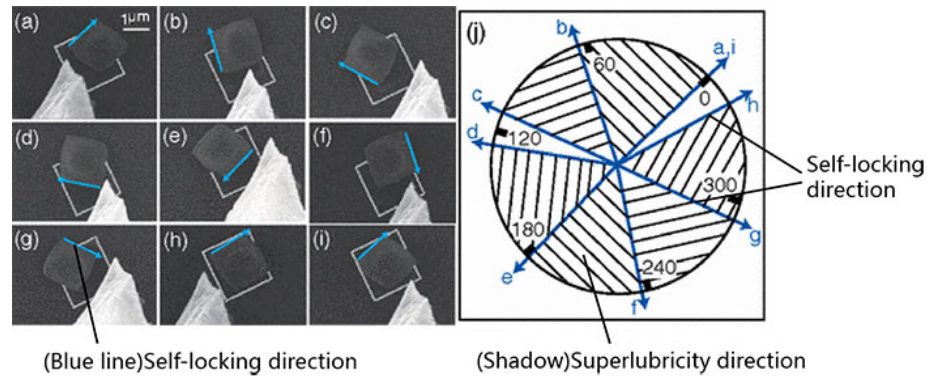
Figure 8. Super-lubrication phenomena beyond the nanometer scale: (**a**–**i**) represent different rotation directions of the graphite sheet, the direction indicated by blue arrow in the figure represents the locking direction, the arrow is always on the same side of graphite sheet, and the square shown by dotted line in the figure represents the graphite platform; (**j**) the locking directions shown in (**a**–**i**) obviously show 60 symmetry, and the scale mark of 0° in this figure is the same as the arrow direction in (**a**) [57].
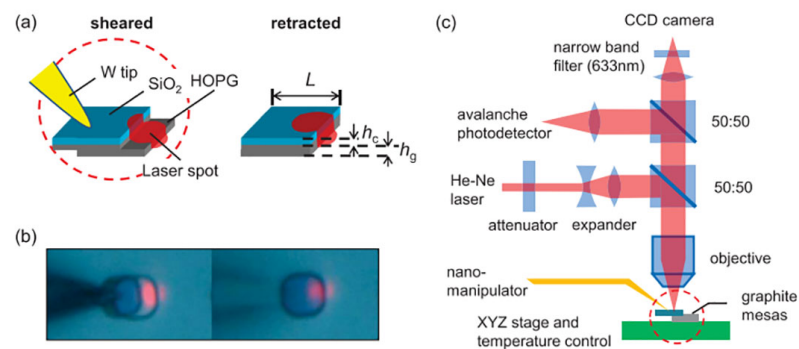
Figure 9. (**a**) Structure of the graphite mesa and the scheme of the manipulation process; (**b**) shearing and retraction under an optical microscope; and (**c**) experimental setup used for optical knife-edge method [58].
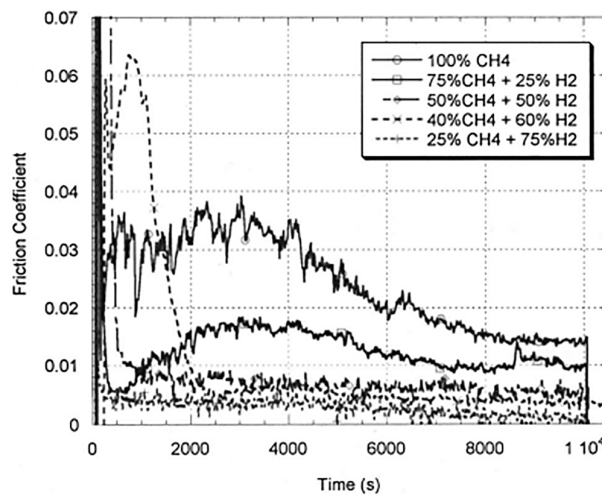
Figure 10. Friction coefficient of DLC films with different hydrogen contents in the deposition process [61].

DLC superlubricity often needs to be realized in inert gas. Many researchers have made different attempts to overcome this shortcoming. Freyman et al. [64] developed a sulfur-doped hydrogenated DLC film, which can maintain an ultra-low friction coefficient of 0.004 in an environment with50% relative humidity because the S-C bond has a higher binding energy. Zhang et al. [65–67] realized the ultra-low friction (friction coefficient is 0.008) of solid lubricating film in an air environment. The a-C:H and a-C: H:Si films prepared by the research group of Tsinghua University Luo Jianbin can achieve a superlubricity state of about 0.001 in the air environment [68]. A novel superlubricity pair was developed by Zhang et al. [69]. They polished the quartz surface with a new environmentally friendly polishing solution, and simultaneously prepared multilayer graphene-deposited quartz spheres, quartz polishing plates, and microspheres with PECVD, which could achieve a superlubricity state with a friction coefficient of 0.006 under room temperature atmospheric conditions (Figure 11), and they concluded that the oscillation and slippage of exfoliated quartz sheets and multilayer graphene-deposited microspheres realized macroscopic superlubricity. Chen et al. [70], members of a research group at Tsinghua University Luo Jianbin, prepared silicon-doped and toughened diamond-like carbon films by using ion beam controlled growth technology, and developed a new robust macroscopic superlubricity system, which achieved an ultra-low friction state with a friction coefficient of 0.006 in an atmospheric humidity environment (Figure 12). It is considered that the nano-silica-like lubricating layer constructed in situ on the surface of the friction pair can effectively shield the tribochemical corrosion of environmental water molecules on the metal surface, and, at the same time, the ordered shearing behavior of adsorbed water molecules induced by the silica-gel lubricating layer in the confined space ensures the superlubricity state.
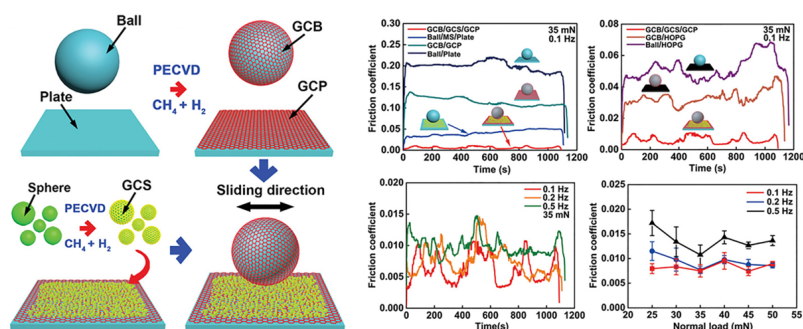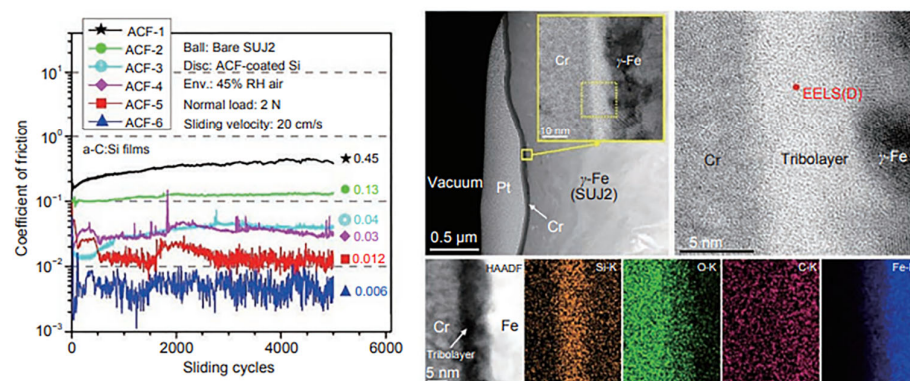

Figure 11. Superlubricity formed by quartz flake with multilayer graphene microspheres [69].

It is worth noting that the superlubricity theory is based on the incommensurability of two crystal planes, so the superlubricity is dependent on the slip direction, that is, it can only be realized in a specific slip direction. In 2017, Tsinghua University Luo Jianbin's research group realized the robust superlubricity of multi-point contact between two-dimensional materials, which was independent of the sliding direction, and solved the problem of the sliding direction dependence of traditional structure superlubricity [71]. The research group used the AFM tip to slide graphite directly, and obtained a friction coefficient of 0.0003 under a contact pressure of 2.52 Gpa [72]. Later, they developed a thermal-assisted mechanical peeling and transfer method, which wrapped different types of two-dimensional materials on the AFM tip so that the tip could directly detect the interlayer coupling, and they achieved a friction coefficient of 10^{-4}~10^{-5}, all of which had nothing to do with the sliding direction [73]. There is still a lot of work being carried out in this field, which will deepen and expand the research on superlubricity [74,75].

Figure 12. Superlubricity formed by the moisture-shielding effect of silicon-doped diamond-like carbon film [70].

2.2.3. Solid–Liquid Combined Superlubricity

The emergence of oil-based liquid superlubricity has greatly expanded superlubricity application, liquid superlubricity in acid (alkali) pumps, water-based lubrication pairs, light-load oil-based friction pairs, etc., but to achieve large-scale application, there are two major defects that need to be overcome. One is that the load-bearing capacity needs to be improved, and hopefully reach the Gpa order of magnitude, and the second is that the use of the conditions needs to be expanded. Two-dimensional materials that are good solid superlubricity materials can also be added to liquids to form solid–liquid coupled superlubricity systems, the main feature in this case being their low shear strength, which makes interlayer sliding more likely to occur. The adsorption of the laminar additives on the surface of the friction pair plays a key role in achieving ultra-low coefficients of friction and ultra-high load-carrying capacity. The most significant advantage of combined solid–liquid superlubricity over single solid/liquid superlubricity is that it avoids strict environmental restrictions while maintaining high load-carrying capacity, which makes it more suitable for practical applications.

In 2018, Wang et al. [76] used sodium hydroxide-modified black phosphorus (BP-OH) added to water as a water-based lubrication additive to achieve superlubricity at the Si_3N_4/sapphire interface. They proved that the exfoliated BP-OH nanosheets formed on the sliding surface prevented the direct contact of rough peaks, and the existence of BP-OH was beneficial to capture water molecules and form a water layer with low shear resistance, thus achieving strong superlubricity under a wide range of contact pressures (1 Gpa). Graphene oxide nanoflakes (GONFs) can interact with ethane diol (EDO) via hydrogen bonding to form a hydrated GONFs-EDO network, and similar results are obtained at the Si_3N_4/SiO_2 interface [77]. Subsequently, in 2019, Ge et al. were able to achieve superlubricity at the Si_3N_4/sapphire interface by incorporating graphene oxide (GO) nanosheets in ionic liquid (Li(EG)PF) at a pressure of 600 MPa [78]. Material surface characterization results showed that graphene oxide nanosheets were absorbed at the wear surface and could withstand high loads while preventing possible adverse reactions. The extremely low shear stress on the interlayer of graphene oxide nanosheets also plays a crucial role in maintaining superlubricity. The processes involved may also occur in aqueous solutions of poly alkyl glycol (PAG) with ultrathin layered double hydroxide nanosheets (ULDH-NSs) [79]. In this case, the absorption of ULDH-NSs on solid surfaces can smooth, polish, and protect the contact due to the relatively low interlayer interactions of ULDH-NSs, and, in addition, the presence of ULDH-NSs facilitates the absorption of PAG.

2.2.4. High-Temperature Superlubricity

Many components in turbines, transportation manufacturing, and aerospace operate at high temperatures. There is an urgent need for lubrication solutions at high temperatures in industrial applications, but high-temperature superlubricity can be very challenging

as many traditional mineral and synthetic oil-based lubricants begin to degrade under high-temperature conditions.

Hexagonal boron nitride is widely used in many fields because of its high thermal conductivity and excellent chemical properties. Studies have found that it also has good lubricity at high temperatures. Zeng deposited h-BN coatings on the surface of high-speed tool steel by radio frequency magnetron sputtering, and investigated the tribological properties of the h-BN coatings in the range of 500~800 °C with a ZrO_2 ball friction pair, and found that the CoFs of the h-BN coatings were much lower than those without coatings under the same conditions [80]. The h-BN coating on the surface of steel exhibits high-temperature superlubricity at 800 °C, and the mechanism is due to the formation of γ-Fe_2O_3/h-BN composite material using friction chemistry. Meanwhile, he also studied the high-temperature superlubricity of the h-BN coating on a textured InconelX750 alloy [81]. Chen et al. prepared SiC/h-BN composites and studied the tribological properties of the composites from room temperature to 900 °C, which showed excellent lubrication properties with a coefficient of 0.30 above 800 °C [82]. Zhao et al. prepared MoO_3-containing composites on Q235 steel and found that a friction chemical film of $CuMoO_4$ was formed during friction, and this transfer film helped to improve the friction reduction performance at a high temperature [83]. Yuan et al. deposited an h-BN coating on a titanium alloy, and the coefficient of friction was reduced from 0.72 to 0.35 [84].

As an ideal sealing material, graphite has self-lubricating properties, high thermal conductivity, excellent chemical stability, and corrosion resistance. Zhang et al. [85] investigated the tribological properties of phenolic resin graphite and a WC-Ni alloy friction pair at different temperatures, and found that the PRG material can achieve ultra-low friction coefficients ranging from 0.01 to 0.015 at 200, 300, and 400 °C, and that the formed graphite friction films interact with each other to form stable friction behaviors and achieve ultra-low friction. It is worth noting that at high temperatures, the oxidation resistance of graphite in atmospheric conditions is relatively poor, and oxidized abrasive particles will change the friction and wear characteristics of graphite. Huai et al. [86] developed a graphite-based solid lubricant filled with SiO2 and investigated the tribological properties of Si_3N_4 balls at 700, 800, and 900 °C. The high-temperature coefficient of friction in atmospheric conditions was about 0.05, and lubrication performance was relatively excellent. Kumar et al. [87] investigated the tribological properties of turbo graphite against a 100Cr6 steel ball in a high-temperature environment, where low coefficients of friction of two-dimensional structural graphite were achieved due to the passivation of the dangling bonds by high absorbed oxygen.

DLC is a common material in the field of tribology, and many researchers have also studied its lubrication ability at high temperatures. Due to poor thermal stability, the ultra-low friction behavior of DLC films is increasingly difficult to achieve under high-temperature conditions, and the change in the friction factor is more complicated with an increase in temperature. Zeng et al. [88] investigated the effect of temperature on the tribological properties of DLC films in the temperature range from ambient to 600 °C, and the lowest stable coefficient of friction (0.008) was observed at 600 °C. They speculated that the ultra-low friction mechanism is a synergistic effect of the shielding effect of hydrogen at the contact surface and the repulsive electrostatic force between the self-generated γ-Fe_2O_3 and SiO_2 composite oxides at the contact surface. Niakan et al. [89] prepared DLC-MoS_2 composite films using the PECVD technique and found that the graphitization rate of the films was slowed down after annealing in air at up to 200 °C with high thermal stability. Alpas et al. [90] prepared W-DLC films and found that the friction factor of the doped W-DLC films was found to be as low as 0.07 and 0.08 at 400 °C and 500 °C, respectively.

Gao et al. [91] achieved high-temperature superlubricity on a nickel high-temperature alloy substrate using antimony trioxide (Sb_2O_3) and magnesium silicate hydroxide coated with carbon (MSH/C). The inner Sb_2O_3 adhesion layer and the top MSH/C layer have a synergistic effect to protect the substrate from sliding in direct exposure to air and also from oxidation. The experimental results show that the friction coefficient of the

coating decreases gradually with an increase in the test temperature, and finally reaches the superlubricity state at 300 °C. The mechanism is that the Sb_2O_3-MSH/C layer avoids direct metal-to-metal contact, thereby preventing the in situ welding of the friction pair and the associated friction spikes. At the same time, the amorphous carbon film generated by friction chemistry and the release of -OH and Si-O active groups also played a role in the realization of high-temperature superlubricity. Wang et al. [92] found that MSH-Sb_2O_3-MoS_2 composite coatings exhibited considerable superlubricity in room temperature experiments and that the friction coefficient of the composite coatings decreased rapidly and eventually reached superlubricity (coefficients <0.01) when the test temperature reached 200 °C and above. The temperature dependence of friction above the water evaporation point was revealed by DSC-TG curve analysis, where an increase in temperature accelerates the destruction of structural water, and its subsequent combination with surface elements directly reduces friction.

At present, in the research field of high-temperature superlubricity, there are many new superlubricity systems being developed, but high-temperature lubrication technology with a coefficient of friction lower than 0.01 is still in its infancy.

3. Mechanism of Superlubricity

3.1. Conditions for the Generation of Superlubricity

Superlubricity denotes a state of interfacial sliding in which friction is extremely low or even disappears. Given that recognizing the source of friction is the basis for suppressing friction or even eliminating friction to achieve superlubricity, it is necessary to briefly discuss the source of friction before introducing the conditions for the generation of superlubricity. Intuitive life experience tells us that the relative sliding friction resistance between rough contact surfaces is large, which is mainly caused by the meshing, deformation, and shearing of rough peaks in the process of relative motion, that is, the classical micro-convex deformation theory of friction origin. In fact, for atomically smooth surfaces with less roughness, or even near-zero physical roughness, frictional resistance still exists and may even be greater when relative sliding occurs. This suggests that there may be other, more intrinsic causes of friction than friction due to the meshing deformation of the physical roughness peaks. Inter-surface adhesion can also significantly affect the frictional behavior of relative sliding, and typically relative sliding between objects with greater adhesion produces greater friction. Accordingly, British scholars proposed the theory of adhesive friction and pointed out that the real cause of friction is the existence of molecular or atomic forces on the friction surfaces. As mentioned above, reducing the physical roughness between the contact surfaces, and realizing weaker interactions between the contact surfaces, such as constructing van der Waals interfaces and blunting surface dangling bonds, may represent effective ways to obtain low friction. Existing methods of realizing superlubricity are closely related to the above-asserted pathways for inhibiting friction generation. Meanwhile, since friction is essentially a process in which mechanical energy is dissipated and converted into other forms of energy, the energy dissipation pathway of friction may be an important cause of friction generation. Based on this, recent scholars have proposed the phonon theory, the potential undulation theory, and the molecular entanglement theory of friction generation from different perspectives, from which effective strategies for realizing superlubricity by controlling friction dissipation have been derived.

Based on current understanding, it is concluded that the following three conditions are required to realize ideal superlubricity [3]: (1) the two surfaces in contact must be crystal planes, even without a step with a single atomic thickness, and the internal stiffness needs to be high enough; (2) the interaction between surface atoms and out-of-plane atoms should be a van der Waals interaction, not a chemical bond; (3) the surfaces are absolutely clean, and there can be no attachments even of an atomic or molecular size. The application of the technology requires a large contact area, and the above three conditions will become very demanding. It can be seen that the road to the application of superlubricity technology in the future will not be smooth and will face many challenges. First of all, it is a great

challenge to achieve a large-area contact surface that meets conditions (1) and (2). For example, it is recognized that monocrystalline silicon, one of the materials that can be processed into the flattest surface of industrial grade, cannot avoid atomic steps. Another kind of material is one with an amorphous surface, such as a diamond-like surface, but this kind of surface has a lot of unsaturated atoms (that is, surface dangling bonds). Even if the physical surface is not a single crystal, the chemical bond at the grain boundary cannot meet the requirement of condition (2).

The rapid development of two-dimensional crystalline materials such as graphene in recent years points to a direction for the preparation of large-size superlubricity materials. The common feature of two-dimensional crystalline materials is that the intrafacial atoms interact with each other through very strong chemical bonds, with very high intrafacial tensile stiffness and strength. Meanwhile, the interlayer atoms are extremely weak physical interactions, that is, van der Waals forces. Therefore, 2D crystalline materials fully satisfy the first two conditions required for superlubricity and are excellent candidates for superlubricity materials. In addition to graphene, other 2D crystalline materials such as molybdenum disulfide (MoS_2), hexagonal boron nitride (h-BN), niobium diene ($NbSe_2$), etc., also have similar properties. However, research on the superlubricity behavior of these materials mainly remains in the theoretical stage. Wang et al. studied the friction behavior of a fluorinated graphene/MoS_2 heterojunction at the atomic level by first principles. Because the lattice parameters of the two two-dimensional crystal materials are different, it is easier to form non-commensurate contact than with the same material, thus forming superlubricity. A similar phenomenon also occurs in the graphene/h-BN system.

To experimentally study the superlubricity behavior of 2D crystalline materials, the first issue that needs to be resolved is the preparation of macroscale 2D crystalline materials, which is one of the current research hotspots in the industry. At the California Institute of Technology, Boyd and others grew graphene at room temperature [93]. In 2014, at South Korea's Samsung Research Institute, Lee et al. [94] prepared wrinkle-free single-crystal graphene with dendrites up to 5cm in size on a germanium substrate. The research also showed that the prepared graphene could be transferred to a silicon dioxide/silicon substrate completely and be wrinkle-free. The research results provide strong support and inspiration for preparing macro-scale super-lubricated surfaces with graphene as the surface layer. Another challenge is to achieve absolutely clean contact between large-scale single-crystal surfaces. Adsorption on the surfaces of two-dimensional crystals cannot be avoided, even in an ultra-clean room. Therefore, a relatively realistic scheme is contact first, and then removal of the adsorbate in the contact area from the contact area using some method. At present, there are two reported methods to remove the adsorbents in the contact area. One is the nano-eraser method proposed by Zheng's team at Tsinghua University [95], in which a small piece of graphite is contacted with graphene, and the adsorbents in front of the movement route are scraped off during the rapid sliding of graphite, which also has a certain removal function for the adsorbents in the contact area. The second method is to wipe two pieces of non-commensurable crystal materials back and forth [96]. With the increase in wiping times, the friction between them decreases rapidly, which shows that the back and forth friction can remove the adsorbents in the interface area, but the research results show that this method cannot meet the "zero" friction standard of superlubricity.

3.2. Unique Properties of Superlubricity

For the rigid sliding system, under low load conditions, the interface sliding can easily avoid the high-energy dissipation of the "stick-slip" sliding mode to achieve continuous sliding, this very low friction state customarily called "superlubricity". Many scholars at home and abroad have made important contributions to the development of this direction. Luo's group discovered several water-based liquid very-low-friction systems [97,98], and Liu and Zhang's group discovered an amorphous, fullerene-carbon film, solid, very-low-friction system [99]. Direct experimental determination of the dissociation energy of graphene in self-retraction motion was independently achieved by E. Koren's

group [100] and Quanshui Zheng's group [101]. Wei Fei and Zhang Yingying [102,103] fixed a several-centimeters-long double-walled carbon nanotube at both ends and hung it in the middle, and then blew it with wind. It was found that a carbon nanotube arc with a "stealth" section was blown out. The carbon nanotubes returned to linear form after the wind was removed, and the blank in the middle disappeared. They hypothesized that this was the discovery of centimeter-scale superlubricity. D. Dietzel and A. Schirmeisen et al. [104] investigated the dependence of friction on the contact area between nano-scale antimony metal particles and HOPG [0001] surfaces in an ultra-high-vacuum environment. Their experimental results indirectly proved that the friction under superlubricity mainly originates from the contact zone boundary. E. Meyer and M. Urbakh's work on single-molecule friction shows that molecular chemical groups at the surface edges constitute another important source of friction during superlubricity [105]. The simulation results of W. K. Kim et al. [106] found that whether or not the superlubricity state can be maintained depends on the relative ratio of the in-plane interaction strengths and the interfacial shear strengths of the slipping surfaces, and the superlubricity state disappears when the in-plane is softer and the interfacial interaction strengths are stronger. M. Urbakh et al. [107] and A. Fasolino et al. [108] have shown through theoretical studies that nano-scale superlubricity is suppressed at high speeds and high temperatures. Since 2012, through the efforts of several national and international groups, more experimental results and theoretical knowledge are now available to understand the nature of superlubricity and its difference toultra-low friction. The unique properties of superlubricity are as follows [3]: (1) The friction between crystal planes with only physical interaction, such as graphene, which is incommensurate and "absolutely" clean contact tends to zero with the decrease in sliding speed. We call this phenomenon "zero" friction. (2) The "zero" friction has nothing to do with the contact area, it can realize the "zero" friction without scale limitation, and "zero" friction can be maintained within a certain range of positive pressure. (3) "Zero" friction brings forward two unique and particularly important characteristics, where the first is zero wear, and the second is zero start–stop friction. (4) For superlubricity with a limited scale, the friction mainly occurs at the edge of the contact zone, which comes from the removal of surface adsorbents (such as water, hydrocarbons, and micro-nano particles) during the sliding process, the dangling bonds of the edge atoms, and the vibration dissipation of the molecular groups dragged by them.

The above behavior of superlubricity is not only different from the usual friction behavior, but also from the behavior of ultra-low friction. In contrast to superlubricity, ultra-low friction, in which the coefficient of friction is extremely small, still has a certain value and cannot tend to zero in physical nature. In addition, ultra-low friction does not have characteristics (2) and (3).

3.3. The Superlubricity Mechanism

3.3.1. Liquid Superlubricity Mechanism

Combined with acid–alcohol system superlubricity, acid and glycerol system super-lubricity, alkali solution superlubricity, etc., three major mechanisms can be summarized to achieve liquid superlubricity, the electric double layer effect [109,110], hydrodynamic effect [111–113], and hydration effect [114–116], as shown in Figure 13, which are also recognized in the world. Sometimes one mechanism can realize superlubricity, and sometimes the joint action of two to three mechanisms is needed [117–120]. Under the support of these three mechanisms, the liquid superlubricity pressure capacity can be increased from about 10 MPa in the past to 300 Mpa. The system is expanded from water-based to solution (acid, alkali, salt), alcohol-based, oil-based, and many other systems, and the friction pair materials are expanded from mica and ceramics to sapphire, metal, DLC film, and so on [121–124].
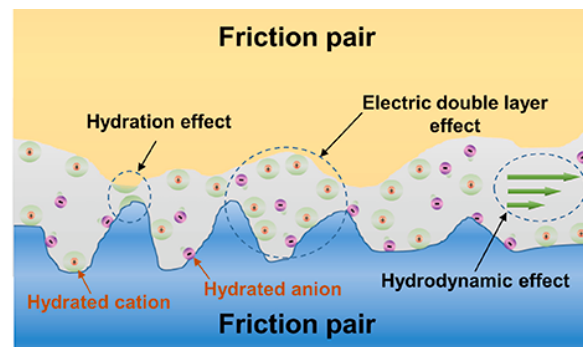
Figure 13. A sketch of the main liquid superlubricity mechanisms [4].

3.3.2. Solid Superlubricity Mechanism

Solid superlubricity mainly comes from the synergistic effect generated by the relative sliding of weakly interacting surfaces in incommensurability contact, and the interfacial atomic synergism can effectively reduce the sliding barrier. It should be pointed out that incommensurability interfaces do not necessarily produce superlubricity with ultra-low friction, and the magnitude of friction is closely related to the degree of incommensurability of the structure, the rigidity of the structure, and the interactions. Although the stacking of incommensurability interfaces can effectively reduce the sliding energy barrier, it also naturally causes the contact between surfaces to be in an unstable state with high potential energy. This unstable structure is prone to structural distortion and deformation under the effect of thermal activation and pollutant adsorption, etc., returning to the local metric contact state, and leading to the destabilization or even loss of superlubricity behavior.

3.3.3. Solid–Liquid Superlubricity Mechanism

The mechanism of action of the solid–liquid combined superlubricity system mainly includes two aspects: the solid phase and the liquid phase. The micro-nano structure on the solid surface is the core of solid–liquid combined superlubricity. By constructing micrometer or nano-scale structures on the solid surface, the actual contact area of the solid surface can be effectively reduced, and the friction between the solid and the liquid can be reduced. At the same time, this micro-nano structure also increases the contact angle of the liquid on the solid surface, making it easier for the liquid to form a slip layer, which further reduces the coefficient of friction. A slip layer is an extremely thin lubricating layer formed by a liquid on a solid surface. When a liquid forms a complete slip layer on a solid surface, the liquid molecules slide across the solid surface, resulting in an ultra-low-friction effect. The formation of the slip layer depends on the nature of the liquid and the micro-nano structure of the solid surface. On the one hand, the lower the viscosity of the liquid, the easier the formation of the slip layer; on the other hand, the more complete the micro-nano structure of the solid surface, the better the stability of the slip layer [125–127].

3.3.4. High-Temperature Superlubricity Mechanism

Most of the high-temperature superlubricity is achieved by composite coatings, in which the mechanisms are very different [128–132]. The low-friction properties of most of these materials at high temperatures are due to the formation of their corresponding oxides. But some materials are different, such as diamond-like carbon films for which superlubricity at high temperatures is mainly due to graphitization. There is usually an intermediate layer between the substrate and the lubricating film. When friction occurs and the lubricating film breaks down, the intermediate layer undergoes a friction chemical reaction at high temperatures to form a composite oxide film [133–135]. The composite oxides have repulsive electrostatic forces between them, which play a role in the realization of high-temperature superlubricity.

4. Superlubricity Material

The concept of superlubricity was proposed by Motohisa Hirano in 1990, but was not confirmed experimentally until 2004. Since then, international research on superlubricity has become increasingly prevalent [136–138]. Two-dimensional materials such as graphene, molybdenum disulfide (MoS_2), and hexagonal boron nitride (h-BN) have become the main materials in the field of superlubricity research due to the unique tribological properties they exhibit at the atomic- and molecular-level scales. Materials that have been demonstrated to exhibit superlubricity under laboratory conditions include graphene, graphite flakes, cubic boron nitride, hydrogen-containing amorphous carbon, molybdenum disulfide, molecular brushes, and ionic liquids [139–143].

In the field of superlubricity, the lubrication mechanism of materials is complex, and its influencing factors are also complex and diverse [144–154]. Under atmospheric conditions, the friction coefficient of graphite/graphite or graphite/steel is about 0.1~0.15, with an obvious friction reduction effect, while in vacuum, the friction coefficient between graphite rises to 0.5~0.8. Similarly, the friction coefficient of MoS_2 cleavage plane and the surface of steel in the atmosphere is only about 0.1, and in vacuum it rises to 0.2, which can be seen as one of the influencing factors of the environment in which the material is located. Graphite produces CO_2 when it comes into contact with oxygen at 325 °C, so it is generally operated at temperatures that do not exceed 400 °C. Graphite is placed in fluorine gas and heated to prepare fluorinated graphite. Under a temperature of 27~345 °C, the friction coefficient of fluorinated graphite is smaller than graphite, and its life is longer than graphite. MoS_2 will oxidize rapidly in 420~430 °C, and when the temperature is more than 800°C, MoS_2 may decompose, and the friction coefficient of molybdenum metal is very large so the lubrication performance is greatly reduced. So, the analysis demonstrated that temperature is also an important factor affecting superlubricity [155–162]. There are also super-lubricant materials that need to be in special gases to have good superlubricity, such as MoS_2, which has good lubricity in dry nitrogen, but poor lubricity in dry oxygen and humid air. DLC films have a much lower coefficient of friction in a hydrogen atmosphere, and if there is no hydrogen in the DLC film, the coefficient of friction is still very high, even when it is protected by a high vacuum or inert gas. There are also, for example, polymer molecular brushes, which can only obtain superlubricity in the surface force apparatus (low speed and low load), and it is difficult to achieve superlubricity in macroscopic (high speed and high load) conditions. This shows that different experimental conditions can also have an effect on the results of achieving superlubricity [163–168]. Researchers from Lanzhou Institute of Chemistry, Chinese Academy of Sciences, also put forward the theory of "pressure-induced superlubricity", which refers to a feasible method to realize superlubricity by increasing pressure induction. The principle is that the wrinkle of a sliding potential energy surface bounces back with the change in normal pressure, and a flat potential energy surface with zero potential energy fluctuation in theory is generated under the critical pressure state, which reduces the sliding energy dissipation to zero in theory. Obviously, the abnormal behavior that its friction decreases with an increase in load reflects that nano-friction is abnormal regarding the macro-friction law and deviates from the intuitive experience of life, which has significant basic research and potential application value.

4.1. Materials for Liquid Superlubricity

The main types of liquid lubrication materials are as follows [169–172]: (1) water-lubricated ceramics—friction chemical reaction on ceramic surfaces when water is used as a lubricant; (2) acid-based liquids—the presence of hydrogen ions and hydrogen bonds is important for superlubricity to occur; (3) ionic liquids—ILs are representative lubricants and lubricant additives that significantly reduce friction and wear, and retard corrosion and mechanical failure; (4) polymer molecular brushes—osmotic pressure is generated between molecular brushes to withstand loads; (5) oil-based liquids—the viscosity of the lubricant has an effect on the coefficient of friction; (6) organism's mucus—this includes human joints, plant mucus, etc.; (7) black phosphorus (BP)—BP is an emerging superlubricity

material. BP nanosheets can be used as an oil-based lubrication additive for solid–liquid combined superlubricity.

4.2. Materials for Solid Superlubricity

The main types of solid lubrication materials are as follows [173–178]: (1) two-dimensional materials—two-dimensional materials with a uniform structure and easy shear provide conditions for the realization of superlubricity, such as molybdenum disulfide and boron nitride; (2) graphite/graphene—both are common solid lubricants, and the incommensurability between the two graphite layers creates conditions for superlubricity to be realized; (3) DLC—the superlubricity of DLC films can be maintained under quite harsh conditions, so it is also the main material used to achieve high-temperature superlubricity, while, at the same time, DLC films are more suitable for macro-scale applications; (4) CNx—the actual carbon nitride content of 12% to 13% of nitrogen in an amorphous structure gives a carbon hardness value of about 30GPa, whichisa CNx coating; (5) h-BN: h-BN—this has a layered crystal structure and excellent properties, and as a solid lubricant, it has a low friction coefficient, and can also be combined with other materials to form a composite material to achieve high-temperature superlubricity; (6) MXenes—MXenes are another relatively new 2D-layered material besides black phosphorus, and in addition to having excellent mechanical strength and flexural rigidity, MXenes have a laminated structure and a low shear strength, resulting in self-lubricating properties, and Ti_3C_2 is one of the most common materials in the MXenes family; (7) high-entropy alloy (HEA)—HEAs consist of at least five elements and have excellent mechanical and tribological properties, making them suitable for antifriction protective films.

5. The Future of Superlubricity Applications

Currently, there are still many constraints for solid-state superlubricity to move towards practical application, such as demanding environmental conditions (vacuum, inert gases, etc.), super-clean and perfect crystal surfaces that are difficult to realize at the macroscopic scale, and the inability to withstand high loads, and so on [179–183]. In contrast, liquid superlubricity is expected to realize engineering applications earlier than solid superlubricity due to relatively low environmental requirements and high load-bearing capacity. In the future, superlubricity will be widely used in aviation, aerospace, transportation, marine vessels, new energy, space agencies, microelectromechanical systems, and other fields [184–188]. At present, the application of superlubricity materials in practice is still focused on the realization of a low friction effect. Regarding ultra-low friction or even zero friction, there is still a long way to go. Here, we present some potentially important applications of superlubricity [189–196].

5.1. Superlubricity in Biomedicine

Tracheal intubation has been widely used in various clinical environments, such as cardiopulmonary resuscitation, respiratory diseases, and anesthesiology. With the help of tracheal intubation, clinicians can control the patient's airway and provide the best conditions for airway patency, oxygen supply, airway suction, and the avoidance of aspiration. However, tracheal intubation is an invasive operation, and the intubation process may cause irritation and damage to the mucosa and tissues of the throat and trachea, and then trigger a series of cardiovascular stress reactions. Although many suggestions and measures have been taken, tracheal intubation may still lead to many complications due to friction. Polymers have been widely used in biomedical engineering, which can greatly improve the tribological properties of objects. Applying this technology to endotracheal tubes can effectively solve the friction problem of endotracheal tubes. A layer of water-soluble biopolymer is combined on the surface of the catheter through a special process, and a lubricating film is quickly formed when it meets water. It has been proved that the superlubricity endotracheal tube can effectively reduce the mechanical stimulation of the trachea to anatomical structures such as the throat, glottis, and trachea, reduce the incidence

of airway injury, shorten the intubation time, and maintain hemodynamic stability during intubation, which is a safe and effective endotracheal intubation tool. By considering this, we can propose the use of superlubricityin biomedical fields, such as for artificial joints and surgical instruments.

5.2. Superlubricity RF MEMS Switches

The RF MEMS switch is the basic core electronic component used to control the on–off state of the circuit. It has the characteristics of a small size, low cost, low energy consumption, low loss, high linearity, and high isolation, and can be widely used in advanced electronic equipment fields such as mobile communication terminals, automated testing, phased array radar, satellite communication, industrial/consumer electrical automation equipment, etc. However, due to the limitations of reliability, operating power, and response time, traditional RF MEMS switches have been unable to achieve large-scale application in related fields. A new electrostatic sliding RF MEMS switch based on structured superlubricity technology developed by Zheng et al. is different to the traditional vertical driving structure. It uses the superlubricity interface to realize signal switching. Because the sliding interface has near-zero friction, no wear, nearly a 100% contact area, and is ultra-lightweight, the new switch will have the characteristics of a long life, high power, and fast response, and will completely break through the main technical bottlenecks of traditional MEMS switches. If the real "ideal switch" is realized, it has the potential to become the biggest breakthrough technological innovation in the electronics industry since the advent of transistors, and to promote the electrification revolution of everything.

5.3. Structured Superlubricity-Based Superpower Storage

With the deepening of digital transformation in all industries, big data, AI, IoT, cloud computing, and the meta-universe have brought about the explosive growth of data and information, and data are no longer just a record of the physical world, but have become a new production source. The ensuing problem is that the increasing amount of massive data requires a large amount of underlying storage space. Storage is at the lowest level of the data development needs, and the data storage capacity demand and market are huge. HDD, as the current mainstream storage method for the data center and cloud storage, is facing technical challenges such as storage density and read/write speed bottleneck. In addition, its flying height has reached its limit, it is very sensitive to vibration, and heat can easily cause lubricating oil volatilization, and large energy consumption and heat dissipation in data centers. In order to solve the above problems, scholars have long proposed the concept of a contact hard disk (i.e., the magnetic head slides on the surface of the platters);however, due to wear and tear problems, contact hard disk technology has always existed only in people's fantasies. In this regard, Zheng Quanshui proposed a super storage device based on structure superlubricity. In view of the fact that the structure superlubricity technology can realize the state of almost zero friction and zero wear when two solid surfaces are in direct contact and relative sliding, it is expected to build the coveted contact hard disk. When the flying height of the magnetic head is reduced to zero, the signal-to-noise ratio is greatly improved, and the storage density and reading and writing speed of the hard disk are increased by 2~3 orders of magnitude. In addition, the contact reading and writing mode also makes the hard disk more resistant to vibration and collision, and it has a higher reliability and longer life. At present, Zheng et al. have completed mechanical principle verification of the ultra-storage device and realized abrasion-free contact sliding verification for up to 100 km in the atmospheric environment by using the structural superlubricity on the hard disk.

5.4. Structured Superlubricity-Based Super Microgenerator

Micro-distributed devices are devices that are small in size (nanometer to millimeter scale), large in number, and distributed to work independently in various application markets. With the rapid development of nanofabrication and micromachining technologies,

micro-distributed devices have a great potential to be used in the next generation of electronics, such as the Internet of Things and micro-robots, to change human life. The number of these miniature devices will be so large and widely distributed that centralizing external power to these devices will be very difficult. So, distributed power self-supply (each device collects its own energy) will be especially important for these micro-devices. The super microgenerator, a device capable of converting weak, low-frequency mechanical or thermal energy from the surrounding physical or biological environment into electrical energy, is characterized by its small structural size and wide range of application. Zheng et al. released the research results of the world's first structural superlubricity super microgenerator in 2021, which is characterized by its small size, simple structure, extremely high energy density, and long lifetime, and it is expected to completely solve the problem of sustained, wireless, and needless replacement of energy supply for the tens of billions of distributed micro- and nano-devices needed for the Internet of Everything.

6. Conclusions and Outlook

Superlubricity, as a brand new branch in the field of tribology, has a wide range of potential applications. In-depth research by scholars from various countries has made great progress, solid superlubricity and liquid superlubricity materials have been widely tapped, and many emerging materials have also joined the study of superlubricity, such as black phosphorus, the Mxenes family, etc.; many classical superlubricity materials have also been explored and new systems have been developed; and high-temperature superlubricity and solid–liquid combined superlubricity have also achieved very significant research results [197–201]. In this article, we introduce the origin and concept of superlubricity to give readers a clear understanding of the importance of superlubricity; categorize and overview the domestic and international research progress of superlubricity; and explore the generation mechanism of various types of superlubricity in the hope of discovering universally applicable mechanisms from a wide range of superlubricity designs. The summary lists classical and novel superlubricity materials, discusses some of the factors affecting the realization of superlubricity, such as temperature, inert gas participation, liquid material addition, etc., and also gives an overview of the future applications of superlubricity that may be widely realized. The current research has found more superlubricity materials and friction sub-materials. There are also many composites and coatings, etc., which were added to achieve an extremely low friction state, but there seems to be no clear understanding of the mechanism of superlubricity generation among them. Further expanding the superlubricity to achieve the correct scale, load-bearing capacity, duration, and reducing the influence of the superlubricity of the factors and the break-in time represent current challenges. From the expansion of the range of materials to the continuous changes in experimental conditions, we are exploring a more systematic mechanism for realizing superlubricity, attempting to reduce the various constraints on the realization of superlubricity, and aiming to tap into more materials capable of realizing superlubricity. Through these studies, we aspire to find simpler systems to realize a durable and stable superlubricity state, so that superlubricity can enter practical applications widely. With the continuous integration of artificial intelligence, machine learning, and simulation, future superlubricity research activities may be able to utilize advanced computational tools and methods to predict and design more reliable and systematic superlubricity systems, discover more new superlubricity materials and surfaces, and thus maximize superlubricity applications, reduce energy loss due to friction and wear, save resources, and bring hope for global sustainability.

References

1. Li, J.; Luo, J. New technology for human getting rid of friction: Superlubricity. *Chin. J. Nat.* **2014**, *36*, 248–255.
2. Erdemir, A.; Martin, J.-M. *Superlubricity*; Elsevier: Amsterdam, The Netherlands, 2007.
3. Zheng, Q.; Ouyang, W.; Ma, M.; Zhang, M.; Zhao, Z.; Dong, H.; Lin, L. Superlubricity: The world of zero friction. *Sci. Technol. Her.* **2016**, *34*, 12–26.
4. Luo, J.; Liu, M.; Ma, L. Origin of friction and the new frictionless technology—Superlubricity: Advancements and future outlook. *Nano Energy* 2021, *prepublish*. [CrossRef]
5. Müser, M.H. Structural lubricity: Role of dimension and symmetry. *Europhys. Lett.* **2004**, *66*, 97–103. [CrossRef]
6. Müser, M.H. Theoretical studies of superlubricity. In *Fundamentals of Friction and Wear on the Nanoscale*; Springer: Cham, Switzerland, 2015; pp. 209–232.
7. Hirano, M.; Shinjo, K. Atomistic locking and friction. *Phys. Rev. B* **1990**, *41*, 11837–11851. [CrossRef]
8. Hirano, M.; Shinjo, K.; Kaneko, R.; Murata, Y. Observation of Superlubricity by Scanning Tunneling Microscopy. *Phys. Rev. Lett.* **1997**, *78*, 1448–1451. [CrossRef]
9. Hirano, M. Atomistics of superlubricity. *Friction* **2014**, *2*, 95–105. [CrossRef]
10. Socoliuc, A.; Bennewitz, R.; Gnecco, E.; Meyer, E. Transition from stick-slip to continuous sliding in atomic friction: Entering a new regime of ultralow friction. *Phys. Rev. Lett.* **2004**, *92*, 134301. [CrossRef]
11. Cahangirov, S.; Ciraci, S.; Özçelik, V.O. Superlubricity through graphene multilayers between Ni(111) surfaces. *Phys. Rev. B* **2013**, *87*, 205428. [CrossRef]
12. Cahangirov, S.; Ataca, C.; Topsakal, M.; Sahin, H.; Ciraci, S. Frictional figures of merit for single layered nanostructures. *Phys. Rev. Lett.* **2012**, *108*, 126103. [CrossRef]
13. Wolloch, M.; Levita, G.; Restuccia, P.; Righi, M.C. Interfacial Charge Density and Its Connection toAdhesion and Frictional Forces. *Phys. Rev. Lett.* **2018**, *121*, 026804. [CrossRef] [PubMed]
14. Zheng, Q.; Liu, Z. Experimental advances in superlubricity. *Friction* **2014**, *2*, 182–192. [CrossRef]
15. Zhou, F.; Wang, X.; Kato, K.J.; Dai, Z. Friction and wear property of a-CNx coatings sliding against Si3N4 balls in water. *Wear* **2007**, *263*, 1253–1258. [CrossRef]
16. Tomizawa, H.; Fischer, T.E. Friction and wear of silicon nitride and silicon carbide in water: Hydrodynamic lubrication at low sliding speed obtained by tribochemical wear. *ASLE Trans.* **1987**, *30*, 41–46. [CrossRef]
17. Long, Y.; Kuwahara, T.; De Barros Bouchet, M.I.; Ristic, A.; Dorr, N.; Lubrecht, T.; Dupuy, L.; Moras, G.; Martin, J.M.; Moseler, M. In situ synthesis of graphene nitride nanolayers on glycerol-lubricated Si3N4 for superlubricity applications. *ACS Appl. Nano Mater.* **2021**, *4*, 2721–2732. [CrossRef]
18. Zhou, F.; Adachi, K.; Kato, K. Friction and wear property of a-CNx coatings sliding against ceramic and steel balls in water. *Diam. Relat. Mater.* **2005**, *14*, 1711–1720. [CrossRef]
19. Chen, M.; Kato, K.; Adachi, K. Friction and wear of self-mated SiC and Si$_3$N$_4$ sliding in water. *Wear* **2001**, *250*, 246–255. [CrossRef]
20. Zhou, F.; Adachi, K.; Kato, K. Sliding friction and wear property of a-C and a-CNx coatings against SiC balls in water. *Thin Solid Films* **2006**, *514*, 231–239. [CrossRef]
21. Xu, J.; Kato, K. Formation of tribochemical layer of ceramics sliding in water and its role for low friction. *Wear* **2000**, *245*, 61–75. [CrossRef]
22. Samanta, S.; Sahoo, R.R. Layer by layer assembled functionalized graphene oxide-based polymer brushes for superlubricity on steel–steel tribocontact. *Soft Matter* **2021**, *17*, 7014–7031. [CrossRef]
23. Klein, J. Hydration lubrication. *Friction* **2013**, *1*, 1–23. [CrossRef]
24. Raviv, U.; Giasson, S.; Kampf, N.; Gohy, J.-F.; Jerome, R.; Klein, J. Lubrication by charged polymers. *Nature* **2003**, *425*, 163–165. [CrossRef] [PubMed]
25. Raviv, U.; Klein, J. Fluidity of bound hydration layers. *Science* **2002**, *297*, 1540–1543. [CrossRef] [PubMed]
26. Klein, J.; Kumacheva, E.; Mahalu, D.; Perahia, D.; Fetters, L.J. Reduction of frictional forces between solid-surfaces bearing polymer brushes. *Nature* **1994**, *370*, 634–636. [CrossRef]
27. Han, T.; Yi, S.; Zhang, C.; Li, J.; Chen, X.; Luo, J.; Banguy, X. Superlubrication obtained with mixtures of hydrated ions and polyethylene glycol solutions in the mixed and hydrodynamic lubrication regimes. *J. Colloid Interface Sci.* **2020**, *579*, 479–488. [CrossRef]

28. Klein, J.; Raviv, U.; Perkin, S.; Kampf, N.; Chai, L.; Giasson, S. Fluidity of water and of hydrated ions confined between solid surfaces to molecularly thin films. *J. Phys. Condens. Matter* **2004**, *16*, S5437–S5448. [CrossRef]

29. Li, J.; Zhang, C.; Luo, J. Superlubricity behavior with phosphoric acid-water network induced by rubbing. *Langmuir* **2011**, *27*, 9413–9417. [CrossRef] [PubMed]

30. Li, J.; Ma, L.; Zhang, S.; Zhang, C.; Liu, Y.; Luo, J. Investigations on the mechanism of superlubricity achieved with phosphoric acid solution by direct observation. *J. Appl. Phys.* **2013**, *114*, 114901. [CrossRef]

31. Li, J.; Zhang, C.; Luo, J. Effect of pH on the liquid superlubricity between Si_3N_4 and glass achieved with phosphoric acid. *RSC Adv.* **2014**, *4*, 23443–23449. [CrossRef]

32. Li, J.; Zhang, C.; Deng, M.; Luo, J. Investigations of the superlubricity of sapphire against ruby under phosphoric acid lubrication. *Friction* **2014**, *2*, 164–172. [CrossRef]

33. Jacques, K.; Joy, T.; Shirani, A.; Berman, D. Effect of water incorporation on the lubrication characteristics of synthetic oils. *Tribol. Lett.* **2019**, *67*, 105. [CrossRef]

34. Wang, W.; He, Y.; Zhao, J.; Mao, J.; Hu, Y.; Luo, J. Optimization of groove texture profile to improve hydrodynamic lubrication performance: Theory and experiments. *Friction* **2020**, *8*, 83–94. [CrossRef]

35. Kuwahara, T.; Romero, P.A.; Makowski, S.; Weihnacht, V.; Moras, G.; Moseler, M. Mechano-chemical decomposition of organic friction modifiers with multiple reactive centres induces superlubricity of ta-C. *Nat. Commun.* **2019**, *10*, 33311–33322. [CrossRef] [PubMed]

36. Zeng, Q.; Yu, F.; Dong, G. Superlubricity behaviors of Si_3N_4/DLC films under PAO oil with nano boron nitride additive lubrication. *Surf. Interface Anal.* **2013**, *50*, 454–465. [CrossRef]

37. Zeng, Q. The Lubrication performances and viscosity behaviors of castor oil under high temperature. *Green Mater.* **2021**, *10*, 51–58. [CrossRef]

38. Ke, L.; Zhang, S.; Liu, D.; Tobias, A.; Zhang, C.; Yuan, C.; Luo, J. Superlubricity of 1,3-diketone based on autonomous viscosity control at various velocities. *Tribol. Int.* **2018**, *126*, 127–132.

39. Li, J.; Zhang, C.; Deng, M.; Luo, J. Achievement of liquid superlubricity of silicone oil by running-in with hydrogen ions. *Nephron Clin. Pract.* **2015**, *54*, 538–541.

40. Yi, S.; Ge, X.; Li, J. Development and prospects of liquid superlubricity. *J. Tsinghua Univ. (Sci. Technol.)* **2020**, *60*, 617–629.

41. Ge, X.; Li, J.; Zhang, C.; Wang, Z.; Luo, J. Superlubricity of 1-ethyl-3-methylimidazolium trifluoromethanesulfonate ionic liquid induced by tribochemical reactions. *Langmuir* **2018**, *34*, 5245–5252. [CrossRef]

42. Han, T.; Zhang, C.; Chen, X.; Chen, X.; Li, J.; Wang, W.; Luo, J. Contribution of a tribo-induced silica layer to macroscale superlubricity of hydrated ions. *J. Phys. Chem. C* **2019**, *123*, 20270–20277. [CrossRef]

43. Fung, Y.C. *Biomechanics: Mechanical Properties of Living Tissues*; Springer: Berlin/Heidelberg, Germany, 1993.

44. Arad, S.; Rapoport, L.; Moshkovich, A.; Moppes, D.; Karpasas, M.; Golan, R.; Golan, Y. Superiorbiolubricant from a species of red microalga. *Langmuir* **2006**, *22*, 7313–7317. [CrossRef]

45. Li, J.; Liu, Y.; Luo, J.; Liu, P.; Zhang, C. Excellent lubricating behavior of Braseniaschreberi mucilage. *Langmuir* **2012**, *28*, 7797–7802. [CrossRef]

46. Du, C.; Yu, T.; Zhang, L.; Deng, H.; Shen, R.; Li, X.; Feng, Y.; Wang, D. Macroscale Superlubricity with Ultralow Wear and Ultrashort Running-In Period (~1 s) through Phytic Acid-Based Complex Green Liquid Lubricants. *ACS Appl. Mater. Interfaces* **2023**, *15*, 10302–10314. [CrossRef] [PubMed]

47. Ma, Q.; Qi, P.; Dong, G. An experimental and molecular dynamics study of the superlubricity enabled by hydration lubrication. *Appl. Surf. Sci.* **2021**, *553*, 149590. [CrossRef]

48. Hirano, M.; Shinjo, K.; Kaneko, R.; Murata, Y. Anisotropy of frictional forces in muscovite mica. *Phys. Rev. Lett.* **1991**, *67*, 2642–2645. [CrossRef] [PubMed]

49. Hirano, M.; Shinjo, K. Superlubricity and frictional anisotropy. *Wear* **1993**, *168*, 121–125. [CrossRef]

50. Martin, J.M. Superlubricity of molybdenum disulphide. *Phys. Rev. B* **1993**, *48*, 10583–10586. [CrossRef] [PubMed]

51. Chhowalla, M.; Amaratunga, G.A.J. Thin films of fullerene-like MoS_2 nanoparticles with ultra-low friction and wear. *Nature* **2000**, *407*, 164–167. [CrossRef]

52. Dienwiebel, M.; Verhoeven, G.S.; Pradeep, N.; Frenken, J.W.M.; Heimberg, J.A.; Zandbergen, H.W. Superlubricity of graphite. *Phys. Rev. Lett.* **2004**, *92*, 126101. [CrossRef]

53. Verhoeven, G.S.; Dienwiebel, M.; Frenken, J.W. Model calculations of superlubricity of graphite. *Phys. Rev. B* **2004**, *70*, 165418. [CrossRef]

54. Robinson, P. Graphite Super Lube Works at Micron Scale. Available online: http://www.rse.org/ehemist:World/2012/05/graphite-super-lube-works-mi-eron-scale (accessed on 28 May 2012).

55. He, G.; Müser, M.H.; Robbins, M.O. Adsorbed layers and the origin of static friction. *Science* **1999**, *284*, 1650–1652. [CrossRef]

56. Müser, M.H.; Wenning, L.; Robbins, M.O. Simple microscopic theory of Amontons's laws for static friction. *Phys. Rev. Lett.* **2001**, *86*, 1295–1298. [CrossRef]

57. Liu, Z.; Yang, J.; Grey, F.; Liu, J.; Liu, Y.; Wang, Y.; Yang, Y.; Cheng, Y.; Zheng, Q. Observation of microscale superlubricity in graphite. *Phys. Rev. Lett.* **2012**, *108*, 205503. [CrossRef] [PubMed]

58. Yang, J.; Liu, Z.; Grey, F.; Xu, Z.; Li, X.; Liu, Y.; Urbakh, M.; Cheng, Y.; Zheng, Q. Observation of high-speed microscale superlubricity in graphite. *Phys. Rev. Lett.* **2013**, *110*, 255504. [CrossRef]

59. Zeng, Q.; Eryilmaz, O.; Erdemir, A. Analysis of plastic deformation in diamond like carbon films–steel substrate system with tribological tests. *Thin Solid Films* **2011**, *519*, 3203–3212. [CrossRef]

60. Erdemir, A. Superlubricity and wearless sliding in diamondlike carbon films. *MRS Proc.* **2001**, *697*, 461–462. [CrossRef]

61. Erdemir, A.; Eryilmaz, O.L.; Fenske, G. Synthesis of diamond like carbon films with superlow friction and wear properties. *J. Vac. Sci. Technol. A* **2000**, *18*, 1987–1992. [CrossRef]

62. Qi, Y.; Konca, E.; Alpas, A.T. Atmospheric effects on the adhesion and friction between non-hydrogenated diamond-like carbon (DLC)coating and aluminum—A first principles investigation. *Surf. Sci.* **2006**, *600*, 2955–2965. [CrossRef]

63. Erdemir, A. The role of hydrogen in tribological properties of diamond-like carbon films. *Surf. Coat. Technol.* **2001**, *146*, 292–297. [CrossRef]

64. Freyman, C.A.; Zhao, B.; Chen, Y.; Chung, Y.-W. Water adsorption and desorption on ultra-low friction sulfur-doped hydrogenated carbon films. *J. Phys. Condens. Matter* **2006**, *18*, 1721–1726. [CrossRef]

65. Zhang, J.; Zhang, B.; Xue, Q.; Wang, Z. Ultra-elastic recovery and low friction of amorphous carbon films produced by a dispersion of multilayer graphene. *Diam. Relat. Mater.* **2012**, *23*, 5–9. [CrossRef]

66. Wang, Z.; Wang, C.; Zhang, B.; Zhang, J. Ultralow friction behaviors of hydrogenated fullerene-like carbon films: Effect of normal load and surfacetribochemistry. *Tribol. Lett.* **2011**, *41*, 607–615. [CrossRef]

67. Wang, C.; Yang, S.; Wang, Q.; Wang, Z.; Zhang, J. Super-low friction and super-elastic hydrogenated carbon films originated from a unique fullerene-likenanostructure. *Nanotechnology* **2008**, *19*, 225709. [CrossRef] [PubMed]

68. Chen, X.; Zhang, C.; Kato, T.; Yang, X.; Wu, S.; Wang, R.; Nosaka, M.; Luo, J. Evolution of tribo-induced interfacial nanostructures governing superlubricity in a-C:H and a-C:H:Si films. *Nat. Commun.* **2017**, *8*, 1675. [CrossRef] [PubMed]

69. Zhang, Z.; Du, Y.; Huang, S.; Meng, F.; Chen, L.; Xie, W.; Chang, K.; Zhang, C.; Lu, Y.; Lin, C.; et al. Macroscale superlubricity enabled by grapheme-coated surfaces. *Adv. Sci.* **2020**, *7*, 1903239. [CrossRef] [PubMed]

70. Chen, X.; Yin, X.; Qi, W.; Zhang, G.; Choi, J.; Wu, S.; Wang, R.; Luo, J. Atomic-scale insights into the interfacial instability of superlubricity in hydrogenated amorphous carbon films. *Sci. Adv.* **2020**, *6*, eaay1272. [CrossRef]

71. Liu, S.; Wang, H.; Xu, Q.; Ma, T.; Yu, G.; Zhang, C.; Geng, D.; Yu, Z.; Zhang, S.; Wang, W.; et al. Robust microscale superlubricity under high contact pressure enabled by graphene-coated microsphere. *Nat. Commun.* **2017**, *8*, 14029. [CrossRef]

72. Li, J.; Luo, J. Superlubricity of graphite sliding against graphene nanoflake under ultrahigh contact pressure. *Adv. Sci.* **2018**, *5*, 1800810. [CrossRef]

73. Liu, Y.; Song, A.; Xu, Z.; Zong, R.; Zhang, J.; Yang, W.; Wang, R.; Hu, Y.; Luo, J.; Ma, T. Interlayer friction and superlubricity in single-crystalline contact enabled by two-dimensional flake-wrapped atomic force microscope tips. *ACS Nano* **2018**, *12*, 7638–7646. [CrossRef]

74. Zeng, Q.; Ning, Z.; Pang, Z.; Wang, Z.; Zheng, C. Self-assembled multilayer WS_2/GO films on amorphous silicon coating for enhancing the lubricating properties. *Appl. Surf. Sci.* **2023**, *624*, 157184. [CrossRef]

75. Zeng, Q.; Ning, Z.; Zhu, J.; Wang, Z.; Pang, Z. A Comparative study on the anti-friction performance of amorphous silicon films enhanced by WS_2 Nanoflakes. *Silicon* **2023**, *15*, 1291–1302. [CrossRef]

76. Wang, W.; Xie, G.; Luo, J. Superlubricity of black phosphorus as lubricant additive. *ACS Appl. Mater. Interfaces* **2018**, *10*, 43203–43210. [CrossRef] [PubMed]

77. Ge, X.; Li, J.; Luo, R.; Zhang, C.; Luo, J. Macroscale superlubricity enabled by the synergy effect of graphene-oxide nanoflakes and ethanediol. *ACS Appl. Mater. Interfaces* **2018**, *10*, 40863–40870. [CrossRef] [PubMed]

78. Ge, X.; Li, J.; Wang, H.; Zhang, C.; Liu, Y.; Luo, J. Macroscale superlubricity under extreme pressure enabled by the combination of graphene-oxide nanosheets withionic liquid. *Carbon* **2019**, *151*, 76–83. [CrossRef]

79. Wang, H.; Liu, Y.; Liu, W.; Liu, Y.; Wang, K.; Li, J.; Ma, T.; Eryilmaz, O.L.; Shi, Y.; Erdemir, A.; et al. Superlubricity of polyalkylene glycol aqueous solutionsenabled by ultrathin layered double hydroxide nanosheets. *ACS Appl. Mater. Interfaces* **2019**, *11*, 20249–20256. [CrossRef]

80. Zeng, Q. High temperature low friction behavior of h-BN coatings against ZrO_2. *Coatings* **2022**, *12*, 1772. [CrossRef]

81. Zeng, Q. High-Temperature Superlubricity Performance of h-BN Coating on the Textured Inconel X750 Alloy. *Lubricants* **2023**, *11*, 258. [CrossRef]

82. Chen, J.; Chen, J.; Wang, S.; Sun, Q.; Cheng, J.; Yu, Y.; Yang, J. Tribological properties of h-BN matrix solid-lubricating composite-sunder elevated temperatures. *Tribol. Int.* **2020**, *148*, 106333. [CrossRef]

83. Zhao, Y.; Feng, K.; Yao, C.; Li, Z. Effect of MoO_3 on the microstructure and tribological properties of laser-clad Ni60/nanoCu/hBN/MoO_3 composite coatings over wide temperature range. *Surf. Coat. Technol.* **2020**, *387*, 125477. [CrossRef]

84. Yuan, S.; Toury, B.; Benayoun, S. Novel chemical process for preparing h-BN solid lubricant coatings on titanium-based substratesfor high temperature tribological applications. *Surf. Coat. Technol.* **2015**, *272*, 366–372. [CrossRef]

85. Zhang, F.; Yin, P.; Zeng, Q.; Wang, J. Insights on the Formation Mechanism of Ultra-Low Friction of Phenolic Resin Graphite at High Temperature. *Coatings* **2021**, *12*, 6. [CrossRef]

86. Huai, W.; Zhang, C.; Wen, S. Graphite-based solid lubricant for high-temperature lubrication. *Friction* **2021**, *9*, 1660–1672. [CrossRef]

87. Kumar, N.; Pandian, R.; Das, P.K.; Ravindran, T.R.; Dash, S.; Tyagi, A.K. High-temperature phase transformation and low frictionbehaviour in highly disordered turbostratic graphite. *J. Phys. D Appl. Phys.* **2013**, *46*, 395305. [CrossRef]

88. Zeng, Q.; Eryilmaz, O.; Erdemir, A. Superlubricity of the DLC films-related friction system at elevated temperature. *RSC Adv.* **2015**, *5*, 93147–93154. [CrossRef]

89. Niakan, H.; Zhang, C.; Hu, Y.; Szupunar, J.A.; Yang, Q. Thermal stability of diamond-like carbon–MoS_2 thin films in different environments. *Thin Solid Films* **2014**, *562*, 244–249. [CrossRef]

90. Banerji, A.; Bhowmick, S.; Alpas, A.T. High temperature tribological behavior of W containing diamond-like carbon (DLC) coating against titanium alloys. *Surf. Coat. Technol.* **2014**, *241*, 93–104. [CrossRef]

91. Gao, K.; Wang, B.; Shirani, A.; Chang, Q.; Berman, D. Macroscale superlubricity accomplished by Sb_2O_3-MSH/C under high temperature. *Front. Chem.* **2021**, *9*, 667878. [CrossRef]

92. Wang, B.; Gao, K.; Chang, Q.; Berman, D.; Tian, Y. Magnesium silicate hydroxide–MoS_2–Sb_2O_3coating nanomaterials for high-temperature superlubricity. *ACS Appl. Nano Mater.* **2021**, *4*, 7097–7106. [CrossRef]

93. Boyd, D.A.; Lin, W.H.; Hsu, C.C.; Teague, M.L.; Chen, C.C.; Lo, Y.Y.; Chan, W.Y.; Su, W.B.; Chen, T.C.; Chang, C.S.; et al. Single-step deposition of high-mobility graphene at reduced temperatures. *Nat. Commun.* **2015**, *6*, 6620. [CrossRef]

94. Lee, J.H.; Lee, E.K.; Joo, W.J.; Jang, Y.; Kim, B.S.; Lim, J.Y.; Choi, S.H.; Ahn, S.J.; Ahn, J.R.; Park, M.H.; et al. Wafer-scale growth of single-crystal monolayer graphene on reusable hydrogen-terminated germanium. *Science* **2014**, *344*, 286–289. [CrossRef]

95. Liu, Z.; Bøggild, P.; Yang, J.; Cheng, Y.; Grey, F.; Liu, Y.; Wang, L.; Zheng, Q. A graphite nanoeraser. *Nanotechnology* **2011**, *22*, 265706. [CrossRef] [PubMed]

96. Ma, M.; Sokolov, I.M.; Wang, W.; Pilippov, A.E.; Zheng, Q.; Urbakh, M. Diffusion through bifurcations in oscillating nano- and microscale contacts: Fundamentals and applications. *Phys. Rev. X* **2015**, *5*, 031020. [CrossRef]

97. Johansson, P.; Elo, R.; Naeini, V.F.; Marklund, P.; Björling, M.; Shi, Y. Insights of the ultralow wear and low friction of carbon fiber reinforced PTFE in inert trace moisture environment. *Tribol. Lett.* **2023**, *71*, 100. [CrossRef]

98. Ma, Z.; Zhang, C.; Luo, J.; Lu, X.; Wen, S. Superlubricity of a mixed aqueous solution. *Chin. Phys. Lett.* **2011**, *28*, 056201.

99. Wei, L.; Zhang, B.; Zhou, Y.; Qiang, L.; Zhang, J. Ultra-low friction of fluorine-doped hydrogenated carbon film with curved graphitic structure. *Surf. Interface Anal.* **2013**, *45*, 1233–1237. [CrossRef]

100. Koren, E.; Lörtscher, E.; Rawlings, C.; Knoll, A.W.; Duerig, U. Adhesion and friction in mesoscopic graphite contacts. *Science* **2015**, *348*, 679–683. [CrossRef]

101. Wang, W.; Dai, S.; Li, X.; Yang, J.; Srolovitz, D.J.; Zheng, Q. Measurement of the cleavage energy of graphite. *Nat. Commun.* **2015**, *6*, 7853. [CrossRef]

102. Zhang, R.; Ning, Z.; Zhang, Y.; Zheng, Q.; Chen, Q.; Xie, H.; Zhang, Q.; Qian, W.; Wei, F. Superlubricity in centimetres-long double-walled carbon nanotubes under ambient conditions. *Nat. Nanotechnol.* **2013**, *8*, 912–916. [CrossRef]

103. Zhang, R.; Ning, Z.; Zhang, Y.; Zhang, Q.; Chen, Q.; Xie, H.; Zhang, Q.; Qian, W.; Wei, F. Optical visualization of individual ultralong carbon nanotubes by chemical vapour deposition of titanium dioxide nanoparticles. *Nat. Commun.* **2013**, *4*, 1727. [CrossRef]

104. Dietzel, D.; Ritter, C.; Mönninghoff, T.; Fuchs, H.; Schirmeisen, A.; Schwarz, U.D. Frictional Duality Observed during Nanoparticle Sliding. *Phys. Rev. Lett.* **2008**, *101*, 125505. [CrossRef]

105. Pawlak, R.; Ouyang, W.; Filippov, A.E.; Razvozov, L.K.; Kawai, S.; Glatzel, T.; Gnecco, E.; Baratoff, A.; Zheng, Q.; Hod, O.; et al. Single-Molecule Tribology: Force Microscopy Manipulation of a Porphyrin Derivative on a Copper Surface. *ACS Nano* **2016**, *10*, 713–722. [CrossRef]

106. Kim, W.K.; Falk, M.L. Atomic-scale simulations on the sliding of incommensurate surfaces: The breakdown of superlubricity. *Phys. Rev. B* **2009**, *80*, 235428. [CrossRef]

107. Filippov, A.E.; Dienwiebel, M.; Frenken, J.W.M.; Klafter, J.; Urbakh, M. Torque and twist against superlubricity. *Phys. Rev. Lett.* **2008**, *100*, 046102. [CrossRef]

108. van den Ende, J.A.; de Wijn, A.S.; Fasolino, A. The effect of temperature and velocity on superlubricity. *J. Phys. Condens. Matter* **2012**, *24*, 445009. [CrossRef]

109. Luo, J.; Deng, M.; Zhang, C. Advances in superlubricity. In Proceedings of the International Tribology Symposium of IFToMM 2017, Jeju, Republic of Korea, 19−22 March 2017.

110. Deng, M. Investigation of Liquid Superlubricity Mechanism. Ph.D. Thesis, Tsinghua University, Beijing, China, 2017. (In Chinese)

111. Luo, J. Advancements and future of tribology from IFToMM. In *Technology Developments: The Role of Mechanism and Machine Science and IFToMM*; Ceccarelli, M., Ed.; Mechanisms and Machine Science; Springer: Dordrecht, The Netherlands, 2011; Volume 1.

112. Li, J.; Zhang, C.; Deng, M.; Luo, J. Investigation of the difference in liquid superlubricity between water- and oil-based lubricants. *RSC Adv.* **2015**, *5*, 63827–63833. [CrossRef]

113. Li, J.; Zhang, C.; Deng, M.; Luo, J. Superlubricity of silicone oil achieved between two surfaces by running-in with acid solution. *RSC Adv.* **2015**, *5*, 30861–30868. [CrossRef]

114. Han, T.; Zhang, C.; Luo, J. Macroscale superlubricity enabled by hydrated alkali metal ions. *Langmuir* **2018**, *34*, 11281–11291. [CrossRef] [PubMed]

115. Han, T.; Zhang, C.; Li, J.; Yuan, S.; Chen, X.; Zhang, J.; Luo, J. Origins of superlubricity promoted by hydrated multivalent ions. *J. Phys. Chem. Lett.* **2020**, *11*, 184–190. [CrossRef] [PubMed]

116. Gnecco, E.; Pawlak, R.; Glatzel, T.; Meyer, E. Atomic-scale investigations of ultralow friction on crystal surfaces in ultrahigh vacuum. In *Superlubricity*; Elsevier: Amsterdam, The Netherlands, 2021; pp. 71–84.

117. Zeng, Q. Superlow friction and diffusion behaviors of a steel-related system in the presence of nano lubricant additive in PFPE oil. *J. Adhes. Sci. Technol.* **2019**, *33*, 1001–1018. [CrossRef]

118. Zeng, Q. Understanding the lubrication mechanism between the polyhydroxyl group lubricants and metal surfaces. *J. Adhes. Sci. Technol.* **2018**, *32*, 1911–1924. [CrossRef]

119. Zeng, Q.; Dong, G. Superlubricity behaviors of Nitinol 60 alloy under oil lubrication. *Trans. Nonferrous Met. Soc. China* **2014**, *24*, 354–359. [CrossRef]

120. Zhu, L.; Dong, J.; Zeng, Q. High temperature solid/liquid lubrication behaviours of DLC films. *Lubr. Sci.* **2021**, *33*, 229–245. [CrossRef]

121. Zhu, J.; Zeng, Q.; Zhang, B.; Yan, C.; He, W. Elevated-temperature super-lubrication performance analysis of dispersion-strengthened WSN coatings: Experimental research and first-principles calculation. *Surf. Coat. Technol.* **2021**, *406*, 126651. [CrossRef]

122. Zhu, J.; Zeng, Q.; Wang, Y.; Yan, C.; He, W. Nano-crystallization driven high temperature self-lubricating properties of magnetron sputtered WS_2 coatings. *Tribol. Lett.* **2020**, *68*, 50. [CrossRef]

123. Zhu, J.; Zeng, Q.; Yan, C.; He, W. WS_2 nanopowders as high-temperature lubricants: An experimental and theoretical study. *ACS Appl. Nano Mater.* **2019**, *2*, 5604–5613. [CrossRef]

124. Zeng, Q.; Cai, S. Low-friction behaviors of Ag-doped γ-Fe_2O_3@SiO_2 nanocomposite coatings under a wide range of temperature conditions. *J. Sol-Gel Sci. Technol.* **2019**, *90*, 271–280. [CrossRef]

125. Zeng, Q.; Erdemir, A.; Erylimaz, O. Ultralow friction of ZrO_2 ball sliding against DLC films under various environments. *Appl. Sci.* **2017**, *7*, 938. [CrossRef]

126. Donnet, C.; Martin, J.M.; Le Mogne, T.; Belin, M. Super-low friction of MoS_2 coatings in various environments. *Tribol. Int.* **1996**, *29*, 123–128. [CrossRef]

127. Zeng, Q.; Dong, G. Influence of load and sliding speed on super-low friction of nitinol 60 alloy under castor oil lubrication. *Tribol. Lett.* **2013**, *52*, 47–55. [CrossRef]

128. Fontaine, J.; Le Mogne, T.; Loubet, J.L.; Belin, M. Achieving superlow friction with hydrogenated amorphous carbon: Some key requirements. *Thin Solid Films* **2005**, *482*, 99–108. [CrossRef]

129. Erdemir, A. Genesis of superlow friction and wear in diamondlike carbon films. *Tribol. Int.* **2004**, *37*, 1005–1012. [CrossRef]

130. Wang, Y.; Gao, K.; Zhang, B.; Wang, Q.; Zhang, J. Structure effects of sp2-rich carbon films under super-low friction contact. *Carbon* **2018**, *137*, 49–56. [CrossRef]

131. Heimberg, J.A.; Wahl, K.J.; Singer, I.L.; Erdemir, A. Superlow friction behavior of diamond-like carbon coatings: Time and speed effects. *Appl. Phys. Lett.* **2001**, *78*, 2449–2451. [CrossRef]

132. Zhu, J.; Zeng, Q.; Zhang, B.; Yan, C.; He, W.; Lin, N. Improving the lubrication of WSNb nanocomposite coatings by the in-situ oxygen shielding effect at elevated temperatures: A combined study with density functional theory simulations. *Proc. Inst. Mech. Eng. Part J J. Eng. Tribol.* **2023**, *237*, 1181–1196. [CrossRef]

133. Deng, M.; Li, J.; Zhang, C.; Ren, J.; Zhou, N.; Luo, J. Investigation of running-in process in water-based lubrication aimed at achieving super-low friction. *Tribol. Int.* **2016**, *102*, 257–264. [CrossRef]

134. Kano, M. Super low friction of DLC applied to engine cam follower lubricated with ester-containing oil. *Tribol. Int.* **2006**, *39*, 1682–1685. [CrossRef]

135. Zeng, Q. Superlow friction of high mileage used oil with CuDTC in presence of MoDTC. *Ind. Lubr. Tribol.* **2017**, *69*, 190–198. [CrossRef]

136. Kano, M.; Martin, J.M.; Yoshida, K.; Bouchet, M.I.D.B. Super-low friction of ta-C coating in presence of oleic acid. *Friction* **2014**, *2*, 156–163. [CrossRef]

137. Erdemir, A.; Eryilmaz, O.L.; Nilufer, I.B.; Fenske, G.R. Synthesis of superlow-friction carbon films from highly hydrogenated methane plasmas. *Surf. Coat. Technol.* **2000**, *133*, 448–454. [CrossRef]

138. Gong, Z.; Shi, J.; Zhang, B.; Zhang, J. Graphene nano scrolls responding to superlow friction of amorphous carbon. *Carbon* **2017**, *116*, 310–317. [CrossRef]

139. Wu, W.; Murashima, M.; Saso, T.; Tokoroyama, T.; Lee, W.Y.; Kousaka, H.; Umehara, N. New in situ superlow-friction method for nitrogen-containing diamond-like carbon coatings using dielectric barrier discharge treatment in ambient air. *Tribol. Int.* **2022**, *174*, 107749. [CrossRef]

140. An, D.; Wang, Z.; Qin, L.; Wu, Y.; Lu, S.; Yang, H.; Ma, Z.; Mawignon, F.G.; Liu, J.; Hao, L.; et al. Preparation of MXene/EP coating for promising anticorrosion and superlow friction properties. *Prog. Org. Coat.* **2023**, *183*, 107779. [CrossRef]

141. Yu, G.; Zhang, Z.; Tian, P.; Gong, Z.; Zhang, J. Macro-scale superlow friction enabled when MoS_2 flakes lubricate hydrogenated diamond-like carbon film. *Ceram. Int.* **2021**, *47*, 10980–10989. [CrossRef]

142. Zeng, Q.; Ning, Z. High-temperature tribological properties of diamond-like carbon films: A review. *Rev. Adv. Mater. Sci.* **2021**, *60*, 276–292. [CrossRef]

143. Li, X.; Xu, X.; Qi, J.; Zhang, D.; Wang, A.; Lee, K.R. Insights into superlow friction and instability of hydrogenated amorphous carbon/fluid nanocomposite interface. *ACS Appl. Mater. Interfaces* **2021**, *13*, 35173–35186. [CrossRef]

144. Yu, G.; Qian, Q.; Li, D.; Zhang, Z.; Ren, K.; Gong, Z.; Zhang, J. The pivotal role of oxygen in establishing superlow friction by inducing the in situ formation of a robust MoS$_2$ transfer film. *J. Colloid Interface Sci.* **2021**, *594*, 824–835. [CrossRef]

145. Sheng, D.; Zhou, J.; Zhang, H.; Tian, H.; Liu, X.; Wang, W.; Qi, X.; Zhang, H. Achievement of super-low friction between ultra-polished quartz lubricated by hydrated hydroxyethyl cellulose. *J. Mater. Eng. Perform.* **2021**, *31*, 1096–1107. [CrossRef]

146. Kuwahara, T.; Long, Y.; De Barros Bouchet, M.I.; Martin, J.M.; Moras, G.; Moseler, M. Superlow friction of a-C: H coatings in vacuum: Passivation regimes and structural characterization of the sliding interfaces. *Coatings* **2021**, *11*, 1069. [CrossRef]

147. Zeng, Q. Thermally induced superlow friction of DLC films in ambient air. *High Temp. Mater. Process.* **2018**, *37*, 725–731. [CrossRef]

148. Yang, Z.; Hu, Z.; Fan, X.; Chen, C. Parallel electricity at friction interface induced fast superlow friction of amorphous carbon films. *Appl. Surf. Sci.* **2022**, *577*, 151962. [CrossRef]

149. Yu, G.; Tian, P.; Ren, K.; Wu, W.; Zhang, Z.; Gong, Z.; Zhang, J. Effects of water molecules on the formation of transfer films and the occurrence of superlow friction. *Ceram. Int.* **2021**, *47*, 21325–21333. [CrossRef]

150. Murashima, M.; Oyama, S.; Kousaka, H.; Tokoroyama, T.; Lee, W.Y.; Umehara, N. New in situ low-friction technology for diamond-like carbon coatings using surface discharge treatment in ambient air. *Tribol. Int.* **2022**, *165*, 107306. [CrossRef]

151. Liu, Y.; Chen, L.; Jiang, B.; Liu, Y.; Zhang, B.; Xiao, C.; Zhang, J.; Qian, L. Origin of low friction in hydrogenated diamond-like carbon films due to graphene nanoscroll formation depending on sliding mode: Unidirection and reciprocation. *Carbon* **2021**, *173*, 696–704. [CrossRef]

152. Berman, D.; Erdemir, A. Achieving ultralow friction and wear by tribocatalysis: Enabled by in-operando formation of nanocarbon films. *ACS Nano* **2021**, *15*, 18865–18879. [CrossRef] [PubMed]

153. Mescola, A.; Paolicelli, G.; Ogilvie, S.P.; Guarino, R.; McHugh, J.G.; Rota, A.; Iacob, E.; Gnecco, E.; Valeri, S.; Pugno, N.M.; et al. Graphene confers ultralow friction on nanogear cogs. *Small* **2021**, *17*, 2104487. [CrossRef] [PubMed]

154. Lu, Y.; Wang, Y.; Huo, F.; Chen, W.; Ma, M.; Ding, W.; He, H.; Zhang, S. Ultralow friction and high robustness of monolayer ionic liquids. *ACS Nano* **2022**, *16*, 16471–16480. [CrossRef] [PubMed]

155. Yin, S.; Wu, H.; Yi, X.; Huang, Z.; Ye, C.; Li, P.; Zhang, Y.; Shi, J.; Hua, K.; Wang, H. Enhanced graphene oxide adhesion on steel surface through boronizing functionalization treatment: Toward the robust ultralow friction. *Carbon* **2023**, *206*, 201–210. [CrossRef]

156. Zeng, Q.; Chen, T. Superlow friction and oxidation analysis of hydrogenated amorphous silicon films under high temperature. *J. Non-Cryst. Solids* **2018**, *493*, 73–81. [CrossRef]

157. da Cruz MG, A.; Budnyak, T.M.; Rodrigues, B.V.M.; Budnyk, S.; Slabon, A. Biocoatings and additives as promising candidates for ultralow friction systems. *Green Chem. Lett. Rev.* **2021**, *14*, 358–381. [CrossRef]

158. Zhang, L.; Xie, G.; Wu, S.; Peng, S.; Zhang, X.; Guo, D.; Wen, S.; Luo, J. Ultralow friction polymer composites incorporated with monodispersed oil microcapsules. *Friction* **2021**, *9*, 29–40. [CrossRef]

159. Shreedharan, S.; Saffer, D.; Wallace, L.M.; Williams, C. Ultralow frictional healing explains recurring slow slip events. *Science* **2023**, *379*, 712–717. [CrossRef] [PubMed]

160. Li, M.; Xiang, Y.; Sun, L.; Zhang, Y.; Yang, W.; Lu, W.; Zhao, X.; Bao, L.; Cai, M.; Yu, B.; et al. Super-wetting interfaces as a multiphase composite prototype for ultra-low friction. *Green Chem.* **2022**, *24*, 7492–7499. [CrossRef]

161. Zeng, Q.; Qin, L. High temperature anti-friction behaviors of a-Si: H films and counterface material selection. *Coatings* **2019**, *9*, 450. [CrossRef]

162. Tan, J.; Guo, Y.; Guo, W. Ultralow friction of ion-containing water nanodroplets. *Nano Res.* **2023**, *16*, 1792–1797. [CrossRef]

163. Li, F.; Chen, L.; Ji, L.; Ju, P.; Li, H.; Zhou, H.; Chen, J. Ultralow friction and corrosion resistant polyurethane/silicone oil composite coating reinforced by functionalized graphene oxide. *Compos. Part A Appl. Sci. Manuf.* **2021**, *148*, 106473. [CrossRef]

164. Yang, J.; Yuan, Y.; Li, K.; Amann, T.; Wang, C.; Yuan, C.; Neville, A. Ultralow friction of 5CB liquid crystal on steel surfaces using a 1,3-diketone additive. *Wear* **2021**, *480*, 203934. [CrossRef]

165. Yu, T.; Shen, R.; Wu, Z.; Du, C.; Shen, X.; Jia, N.; Deng, H.; Zhao, Y.; Zhang, L.; Feng, Y.; et al. Monolayer NbSe$_2$ Favors Ultralow Friction and Super Wear Resistance. *Nano Lett.* **2023**, *23*, 1865–1871. [CrossRef]

166. Ren, K.; Yu, G.; Zhang, Z.; Wu, W.; Tian, P.; Chhattal, M.; Gong, Z.; Li, Y.; Zhang, J. Self-organized transfer film-induced ultralow friction of Graphene/MoWS4 heterostructure nanocomposite. *Appl. Surf. Sci.* **2022**, *572*, 151443. [CrossRef]

167. Jeong, H.; Hong, S.J.; Kyeong, J.S.; Lee, K.Y.; Han, B. First-principles design of an ultralow frictional interface of a black phosphorus and graphene heterostructure with oxide functionalization and high-pressure conditions. *Appl. Surf. Sci.* **2023**, *608*, 155092. [CrossRef]

168. Liu, W.; Wang, K.; Song, J.; Zhang, L.; Liu, Y. Ultralow friction of basil-based gel in the presence of ethanol as a green lubricant for biomedical applications. *Tribol. Int.* **2022**, *165*, 107320. [CrossRef]

169. Zeng, Q.; Cai, S.; Li, S. High-temperature low-friction behaviors of γ-Fe$_2$O$_3$@SiO$_2$ nanocomposite coatings obtained through sol–gel method. *J. Sol-Gel Sci. Technol.* **2018**, *85*, 558–566. [CrossRef]

170. Pan, J.; Liu, C.; Gao, X.; Zhang, K.; Zheng, W.; Chen, C. Dual-phase nanocomposite TiB2/MoS1. 7B0. 3: An excellent ultralow friction and ultralow wear self-lubricating material. *ACS Appl. Mater. Interfaces* **2021**, *13*, 59352–59363. [CrossRef]

171. Avilés, M.D.; Carrión, F.J.; Sanes, J.; Bermúdez, M.D. Bio-based ionic liquid crystal for stainless steel-sapphire high temperature ultralow friction. *Wear* **2021**, *484*, 204020. [CrossRef]

172. Chen, H.; Zhang, L.; Li, M.; Ren, Y.; Xie, G. Ultralow friction polymer composites containing highly dispersed and thermally robust microcapsules. *Colloids Surf. A Physicochem. Eng. Asp.* **2022**, *634*, 127989. [CrossRef]

173. Li, L.; Zhang, H.; Pan, Y.; Ju, X.; Tang, L.; Li, M. Influence of stress wave-induced disturbance on ultra-low friction in broken blocks. *Int. J. Coal Sci. Technol.* **2022**, *9*, 22. [CrossRef]

174. Chen, W.; Fu, X.; Cao, L.; Gao, S.; Wan, Y. Ultralow friction of copper by a green water-based lubricant containing phytic acid. *J. Mol. Liq.* **2021**, *338*, 116704. [CrossRef]

175. Sun, W.; Ye, J.; Song, Q.; Feng, Y.; Liu, X. Ultralow friction PTFE/PEEK heterolayer: A new solid lubrication approach toward simplicity. *Friction* **2023**, *12*, 120–135. [CrossRef]

176. Li, H.; Branicio, P.S. Ultralow friction of graphene-coated silica nanoparticle film. *Comput. Mater. Sci.* **2022**, *204*, 111184. [CrossRef]

177. Shi, B.; Gan, X.; Lang, H.; Zou, K.; Wang, L.; Sun, J.; Lu, Y.; Peng, Y. Ultra-low friction and patterning on atomically thin MoS 2 via electronic tight-binding. *Nanoscale* **2021**, *13*, 16860–16871. [CrossRef]

178. Ellinas, K.; Gogolides, E. Ultra-low friction, superhydrophobic, plasma micro-nanotextured fluorinated ethylene propylene (FEP) surfaces. *Micro Nano Eng.* **2022**, *14*, 100104. [CrossRef]

179. Kumar, A. Advancements in emerging superlubricity: A review of the atomistic models, simulation techniques and their applications to explore the state of ultra-low friction. *Mater. Today Proc.* **2021**, *42*, 884–892. [CrossRef]

180. Pathak, S.; Zhang, R.; Gayen, B.; Kumar, V.; Zhang, H.; Pant, R.P.; Wang, X. Ultra-low friction self-levitating nanomagnetic fluid bearing for highly efficient wind energy harvesting. *Sustain. Energy Technol. Assess.* **2022**, *52*, 102024. [CrossRef]

181. Li, Q.; Su, F.; Chen, Y.; Sun, J. From ultra-low friction to superlubricity state of black phosphorus: Enabled by the critical oxidation and load. *Friction* **2023**, *11*, 1829–1844. [CrossRef]

182. Yuan, S.; Zhang, C. A sulfonated modification of PEEK for ultralow friction. *Friction* **2023**, *11*, 881–893. [CrossRef]

183. Yu, W.; Liu, J.; Yang, Y.; Hao, J.; Xu, L. An ultralow-friction, low-temperature-lubrication, anti-volatilization and anti-corrosion organohydrogel merely containing nanosilicagelator. *Tribol. Int.* **2023**, *180*, 108302. [CrossRef]

184. Xu, Y.; Zhu, X.; Cheng, Z.; Lu, Z.; He, W.; Zhang, G. A novel ultra-low friction heterostructure: Aluminum substrate-honeycomb borophene/graphene heterojunction. *Comput. Mater. Sci.* **2022**, *205*, 111236. [CrossRef]

185. Chen, W.; Xu, B.; Tang, Q.; Qian, S.; Bian, D.; Li, H. Preparation and Properties of PDMS Surface Coating for Ultra-Low Friction Characteristics. *Langmuir* **2023**, *39*, 14605–14615. [CrossRef]

186. Li, Z.; Wang, B.; Xu, Q.; You, D.; Li, W.; Wang, X. A dual-crosslinked zwitterionic hydrogel with load-bearing capacity and ultra-low friction coefficient. *Mater. Chem. Phys.* **2023**, *307*, 128208. [CrossRef]

187. Zhang, Z.; Yu, G.; Geng, Z.; Tian, P.; Ren, K.; Wu, W.; Gong, Z. Ultra low friction of conductive carbon nanotube films and their structural evolution during sliding. *Diam. Relat. Mater.* **2021**, *120*, 108617. [CrossRef]

188. Chen, F.; Yan, K.; Hong, J.; Song, J. Synergistic effect of graphene and β-Si$_3$N$_4$ whisker enables Si$_3$N$_4$ ceramic composites to obtain ultra-low friction coefficient. *Tribol. Int.* **2023**, *178*, 108045. [CrossRef]

189. Wang, Y.; Li, D.; Shang, L.; Wang, F. Ultra-low friction of ascorbic acid as polyethylene glycol additive in graphite-like carbon film/bearing steel interface. *Diam. Relat. Mater.* **2023**, *135*, 109882. [CrossRef]

190. Li, F.; Chen, L.; Ma, Y.; Ji, L.; Zhou, H.; Chen, J. Sweating-like engineered ultra-low friction coating by a template assisted method. *Tribol. Int.* **2023**, *189*, 109006. [CrossRef]

191. Qi, W.; Xiao, L.; Yu, Q.; Chen, X.; Jin, J.; Yang, J.; Wu, S. Tribolayer-dependent origin of ultralow friction in nanocrystalline diamond films sliding against Si$_3$N$_4$ ball. *Surf. Interface Anal.* **2021**, *53*, 919–932. [CrossRef]

192. Liu, N.; Gao, J.; Xu, L.; Wan, Y.; Li, R. Effect of Carbon Target Current on Ultralow Frictional Behavior of CrCN Coatings under Glycerol Lubrication. *Coatings* **2021**, *11*, 1155. [CrossRef]

193. Xu, Y.; Zhu, X.; Cheng, Z.; Lu, Z.; He, W.; Zhang, G. Effect of strain on the tribological properties of honeycomb borophene/graphene heterostructures: An electronic hierarchical understanding of ultra-low friction. *Tribol. Int.* **2022**, *174*, 107707. [CrossRef]

194. Xu, Y.; Cheng, Z.; Zhu, X.; Lu, Z.; Zhang, G. Ultra-low friction of graphene/honeycomb borophene heterojunction. *Tribol. Lett.* **2021**, *69*, 44. [CrossRef]

195. He, H.; Mu, J.; Mu, J.; Feng, C.; Zhao, J.; Wang, Y.; Zhou, H.; Zhang, L.; He, J.; Chou, X. Breeze-activated wind speed sensor with ultra-low friction resistance for self-powered gale disaster warning. *Sci. China Technol. Sci.* **2023**, *66*, 57–70. [CrossRef]

196. Yan, W.; Zhang, Z.; Zhang, Y.; Chen, L.; Zhang, X.; Liao, B.; Ying, M. Research on Ti-GLC/TiCN/TiN composite multilayer coating with ultra-low friction coefficient in various environments. *Surf. Interfaces* **2021**, *26*, 101426. [CrossRef]

197. Shi, J.; Zhao, R.; Ke, S.; Wang, W.; Wang, C. Probing the ultra-low friction mechanism of hydrogenated carbon films with controllable fullerene-like nano-structures grown with different bias voltage. *Tribol. Int.* **2022**, *175*, 107796. [CrossRef]

198. Sun, L.; Jia, Q.; Zhang, B.; Gao, K.; Tan, X.; Lai, Z.; Zhang, J. Achieving ultra-low friction of a-C: H film grown on 9Cr18Mo steel for industrial application via programmable high power pulse magnetron sputtering. *Surf. Interface Anal.* **2022**, *54*, 81–91. [CrossRef]

199. Kabengele, T. A Study of Ultra-Low Friction in Two-Dimensional Materials Using Density-Functional Theory. Master's Thesis, Dalhousie University, Halifax, NS, Canada, 2021.

200. Khadem, M.; Hwang, Y.H.; Penkov, O.V.; Kim, D.E. Ultralow Macroscale Friction and Wear of MoS$_2$ in High-Vacuum Through DC Pulsing Optimization, Nitridization, and Sublayer Engineering. *Adv. Mater. Interfaces* **2022**, *9*, 2201412. [CrossRef]
201. Zeng, Q.; Dong, G.; Martin, J.M. Green superlubricity of Nitinol 60 alloy against steel in presence of castor oil. *Sci. Rep.* **2016**, *6*, 29992. [CrossRef] [PubMed]